A REVIEW OF RECENT LABORATORY AND NUMERICAL SIMULATIONS OF CUMULUS FLOWS

RODDAM NARASIMHA

Jawaharlal Nehru Centre for Advanced Scientific Research, Bangalore

22 January 2013

Workshop on Clouds, Climate, and Tropical Meteorology

International Centre for Theoretical Sciences

CO-AUTHORS / COLLEAGUES / STUDENTS . . .

Including in particular (in rough anti-chronological order):

K R Sreenivas
G S Bhat
S Diwan
S M Deshpande
P Kulkarni
Vybhav Rao
P Prashanth
D Subrahmanyam
Aditya Konduri
L Venkatkrishnan
A J Basu

Sponsors :

Intel, Bangalore
Computing Research Labs, Pune
Department of Science & Technology
Defence Research & Development Organisation
US Office of Naval Research

NATURAL AND LABORATORY CLOUDS

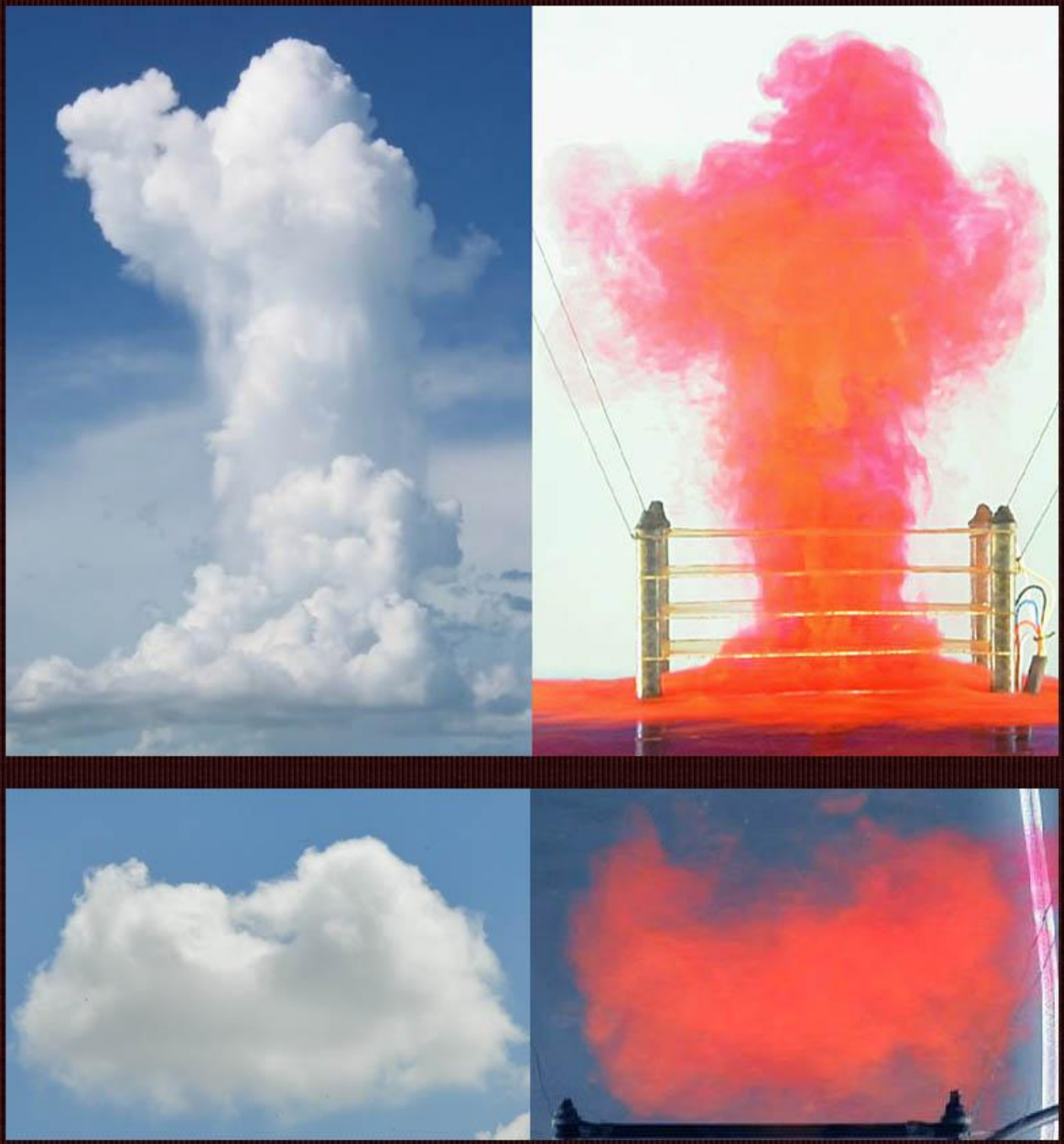

Cumulus congestus

Cumulus flow is a transient diabatic plume

Cumulus mediocris

RN ++ 2011 *PNAS*

MOVIE

Arizona cloud movie 11_09_23 (taken on aug_16_02).mov

CLOUD LIFE-TIMES

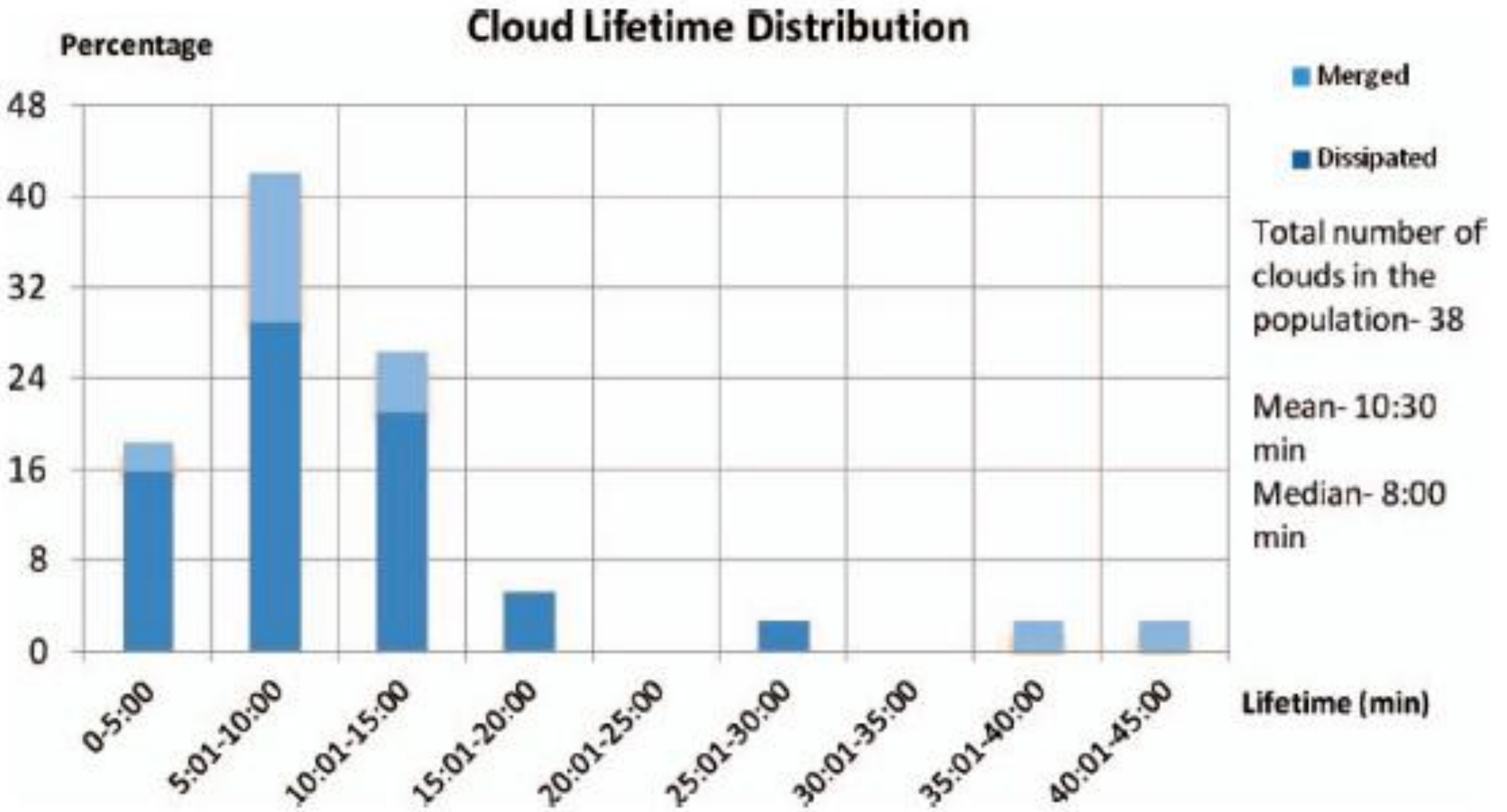

Figure 1. Distribution of cloud life times, as estimated from the time-lapse cloud movies on the Arizona State University website [16].

THE APPARATUS

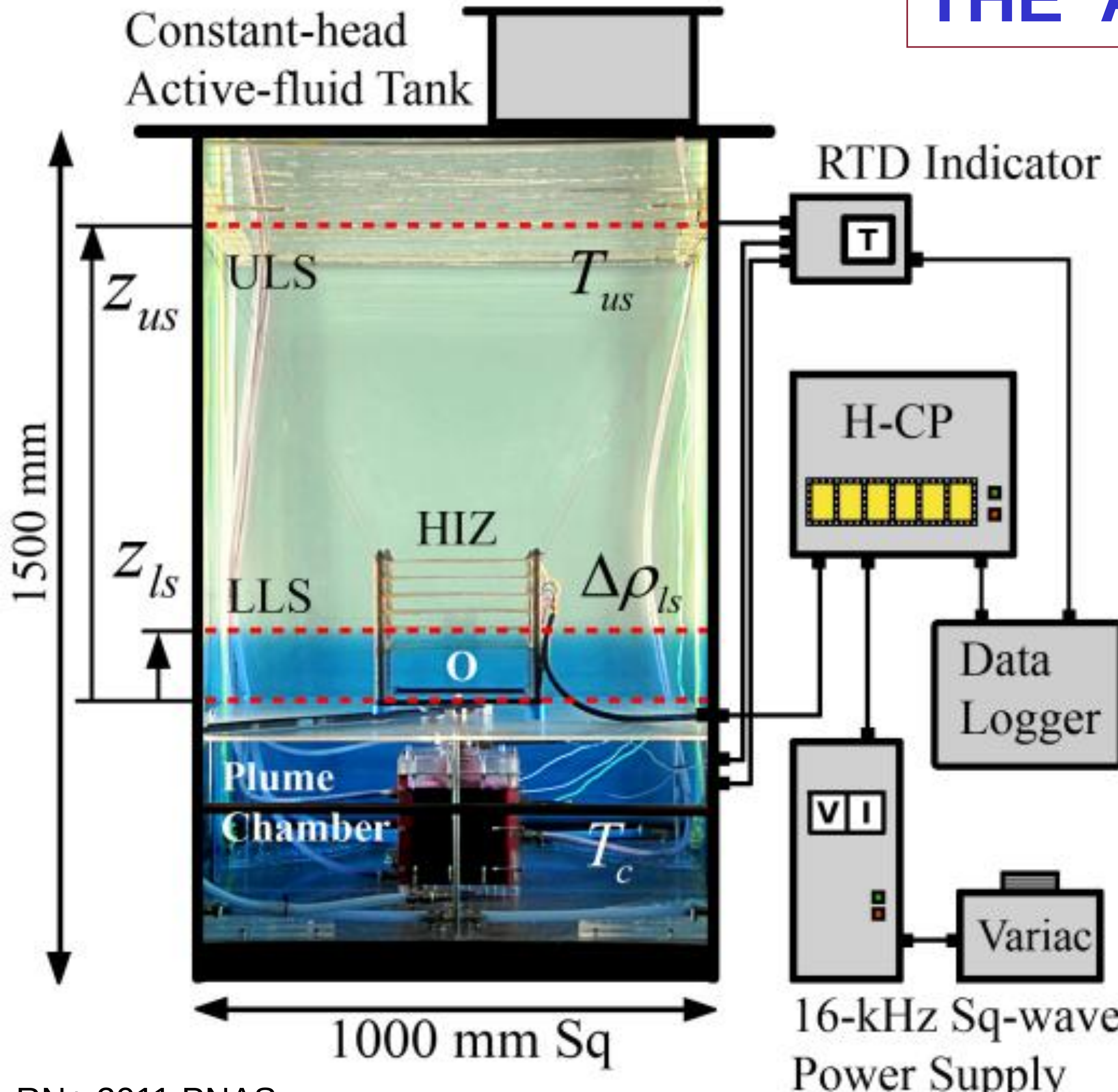

ULS: Upper level stratification
LLS: Lower level stratification
HIZ: Heat injection zone
O: Orifice
RTD: Resistance thermometer
H-CP: Heat control panel
T: Temperature
$\Delta\rho$: Density difference
X_{us}: X at upper stratification
$X_{L}s$: X at lower stratification
X_c: X at plume chamber
VI: Voltage, current

Electrodes

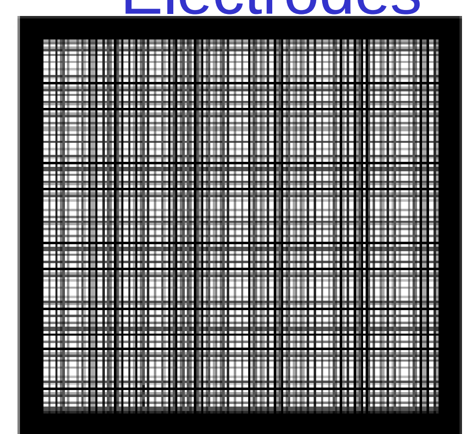

RN+ 2011 PNAS

CLASSICAL IDEAS DO NOT WORK

- Clouds are complex flows involving multiple phases, thermodynamics, microphysics, radiation . . . ? ?
- A central problem in the fluid dynamics of clouds concerns their entrainment characteristics; **entrainment is also the dynamic behind shape**
- Taylor’s entrainment hypothesis for free turbulent shear flows (Morton, Taylor, Turner 1956):
  entrainment velocity $V_e \propto$ characteristic mean velocity U_c
  Later refinements: replace U_c by
  u'_c, $(u' w')^{1/2}$ etc.
- Often works well (Turner 1973, 1986 JFM)
- Suggest constant entrainment coefficient

$$\alpha_E = (dm/dz) \; / \; 2\pi\rho b U_c \bigstar$$

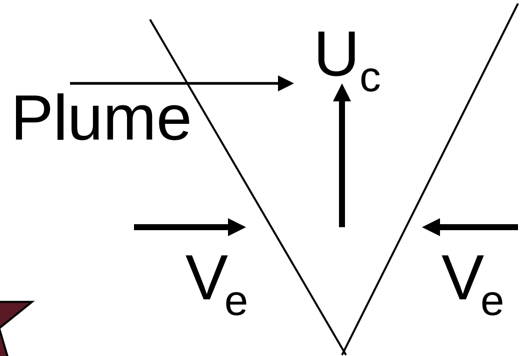

PHYSICAL FLOW MODELS

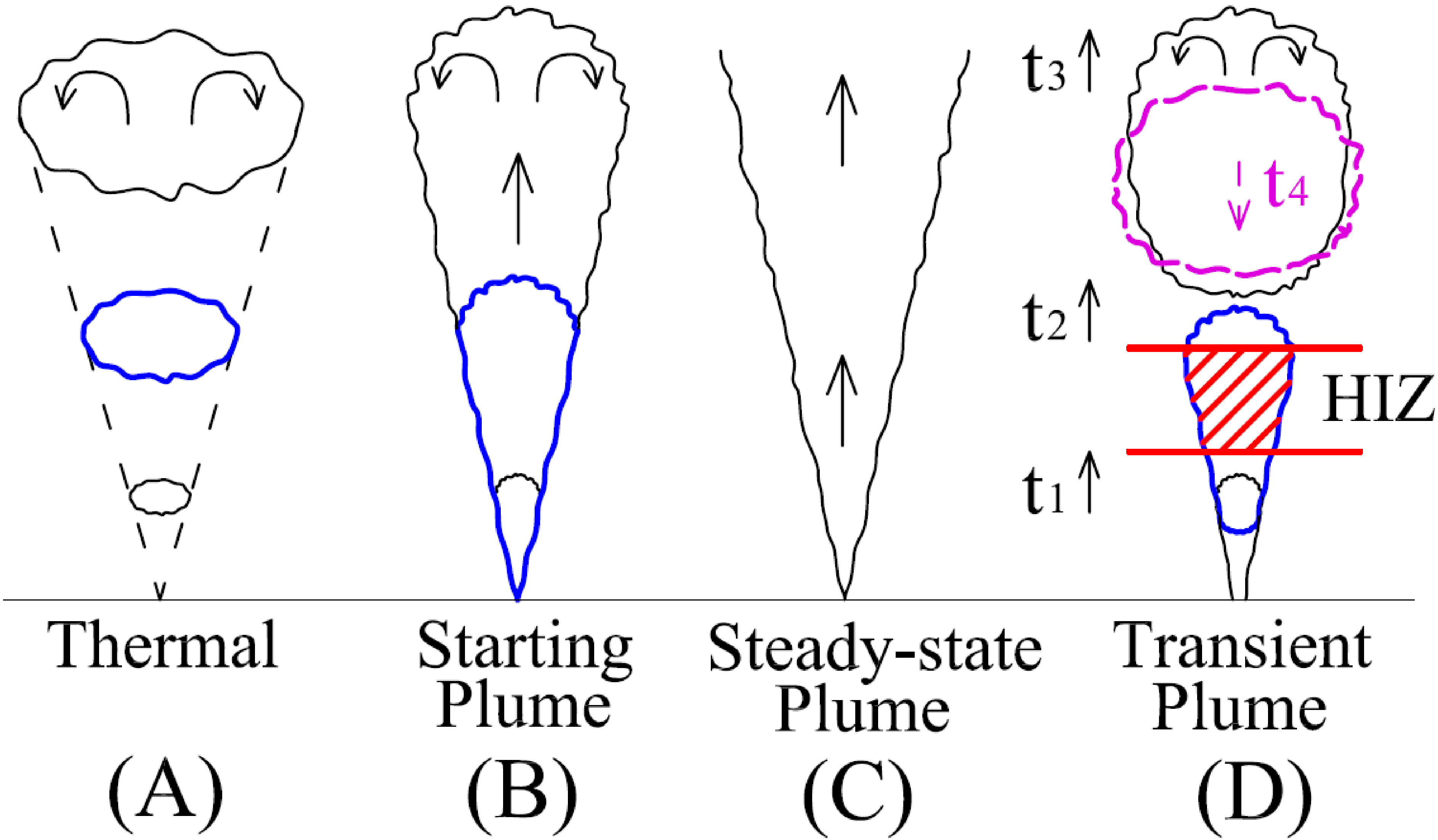

DYNAMICAL SIMILARITY

$$G = \frac{Q}{b_b U_b^3} \frac{g\beta}{\rho_o C_p}, \tag{8}$$

where C_p is specific heat at constant pressure, Q the total off-source volumetric heat put into the flow, and b_b and U_b are, respectively, characteristic length and velocity scales, for example, at condensation level in the cloud or the beginning of heat generation in the apparatus. In the atmospheric cloud Q is O (1 W/m^3) [41] and $G = 0.1$–2 [42]. The same range of values of G can be obtained in water subjected to a heating rate of order 4 MW/m^3, which over a volume of order 250 cm^3 is a manageable 1–2 kW.

CUMULUS CONGESTUS

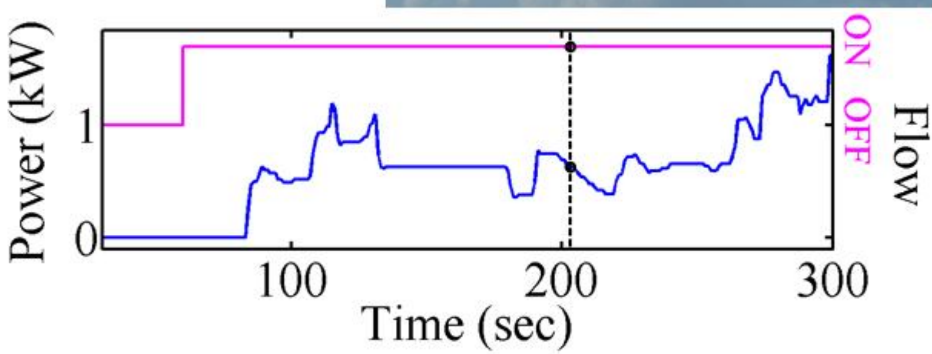

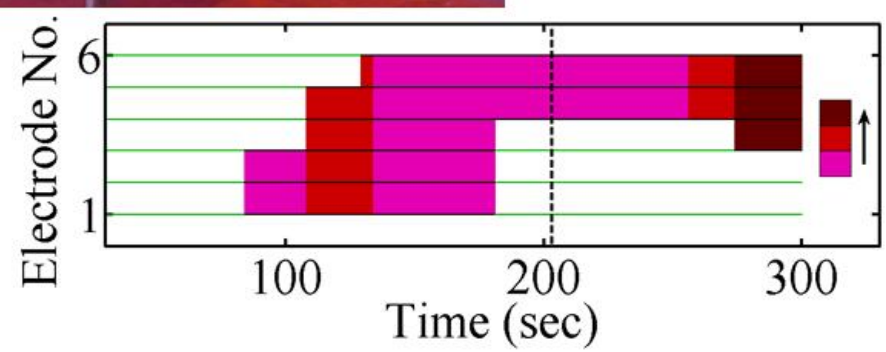

$Re \approx 3000$	$T_c = 30.8^o\mathrm{C}$	$T_{us} = 33.9^o\mathrm{C}$	$\Delta\rho_{ls} \approx 1\mathrm{kg/m^3}$	$z_{ls} = 126.5\mathrm{mm}$	$z_{us} = 869\mathrm{mm}$

REAL CLOUDS, LAB CLOUDS

EMU, JNCASR

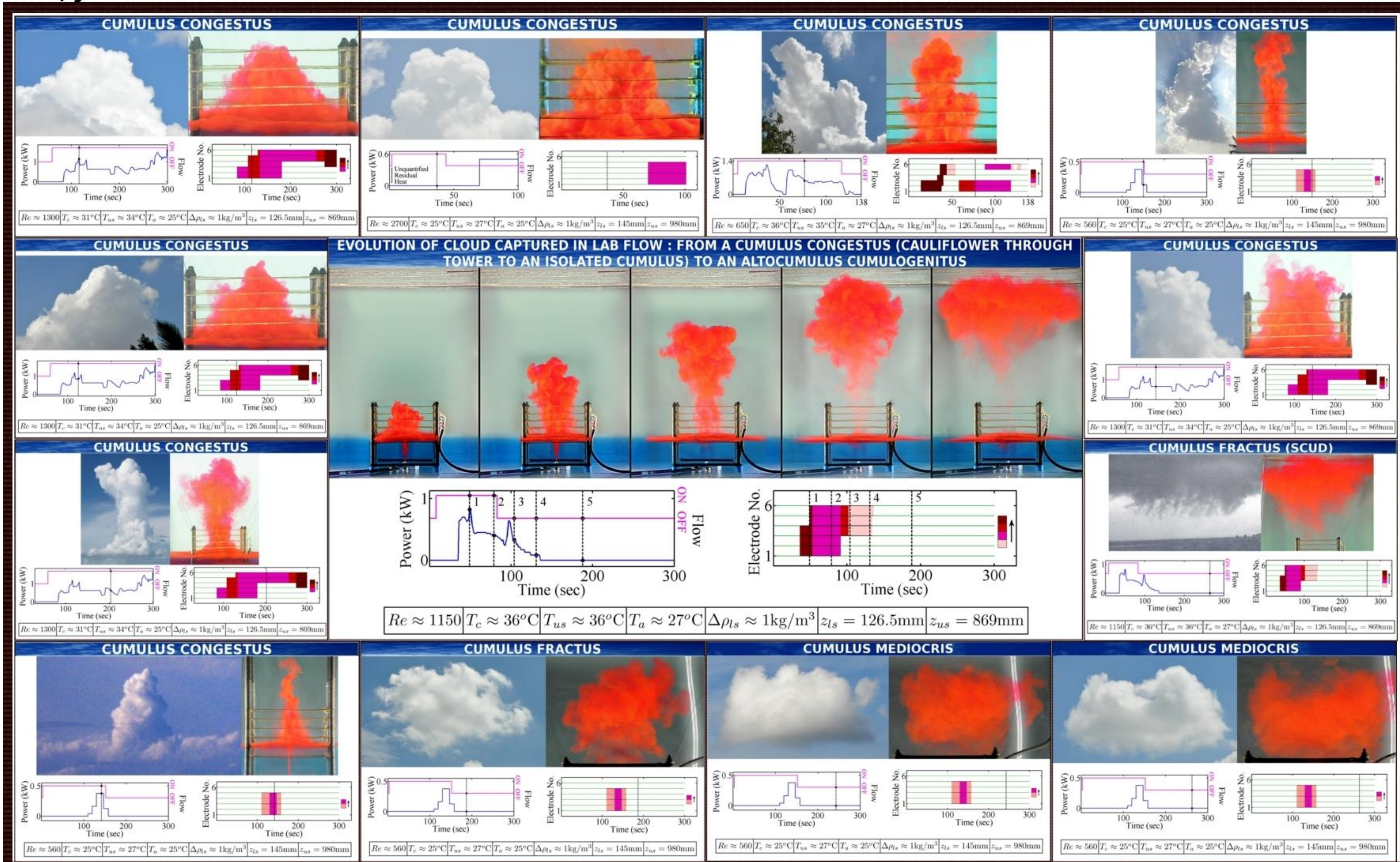

Heat Release causes 'Structural' Changes

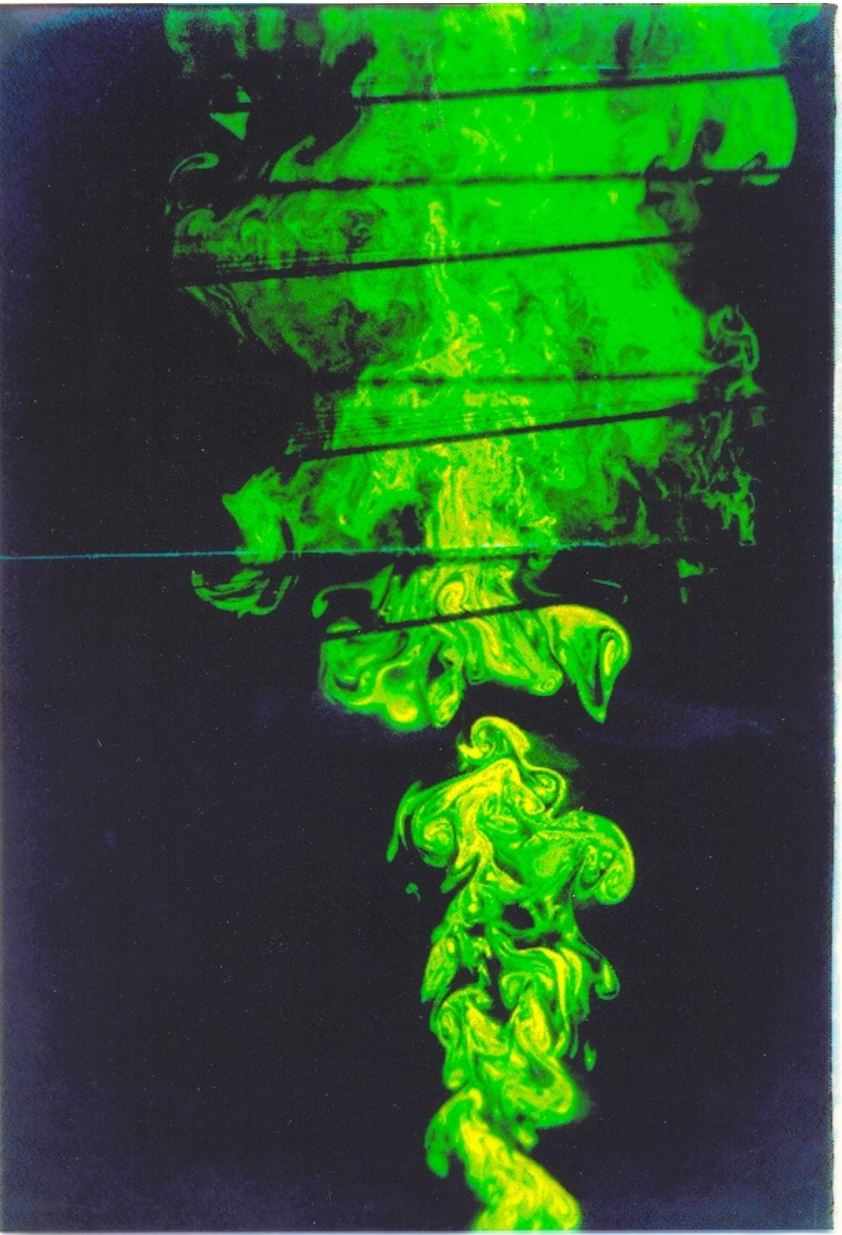

Plume with off-source heating

Off-source heat generation
begins here

Canonical plume

Venkatakrishnan et al. 1998
Curr. Sci.

A COLLAGE : STEADY DIABATIC JETS

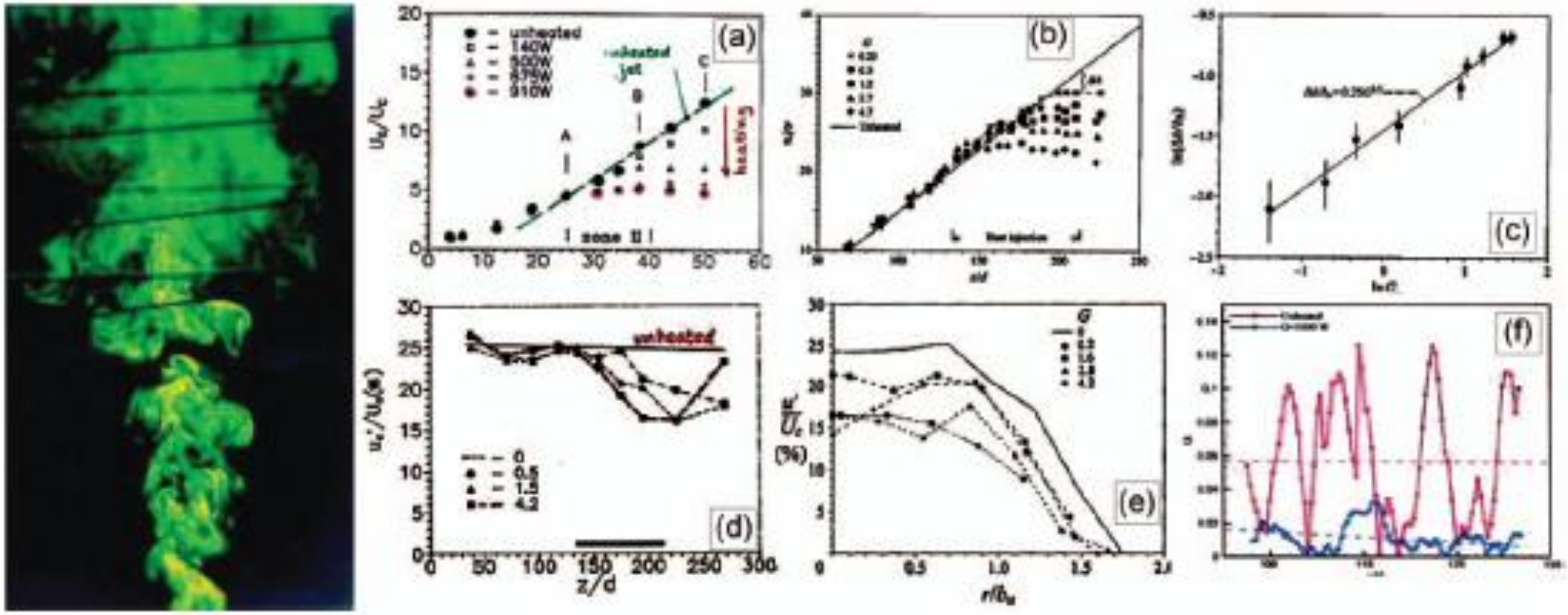

Figure 3. A collage of diagrams summarizing the most striking features of steady diabatic plumes and jets. (Photograph on left) PLIF image of diabatic plume [47], showing the dramatic change in the turbulent structure of the plume almost immediately after the beginning of the heat release slightly above the halfway mark in the photograph. Note the hole in the non-diabatic plume a little below the halfway mark. The picture suggests a 'mixedness transition' due to volumetric heat release. (a) Variation of the reciprocal of the centerline velocity with height at different amounts of heat release (BhN). (b) Streamwise variation of scalar jet width at different values of the heat release parameter G (BhN). (c) The reduction in width shown in (b), as a function of G, increasing like $G^{1/2}$ (BhN). (d) Normalized value of the streamwise turbulence intensity at the centerline (BhN). (e) Radial variation of the normalized streamwise turbulence intensity at $z/d = 225$ at different values of G (BhN). (f) Spatial variation of the entrainment coefficient with and without diabatic heating [46]. Left: Reproduced with permission from [47]. (a)-(e): Reproduced with permission from [40]. (f): Reproduced with permission from [46].

Effect of Off-source Heating on a Plume

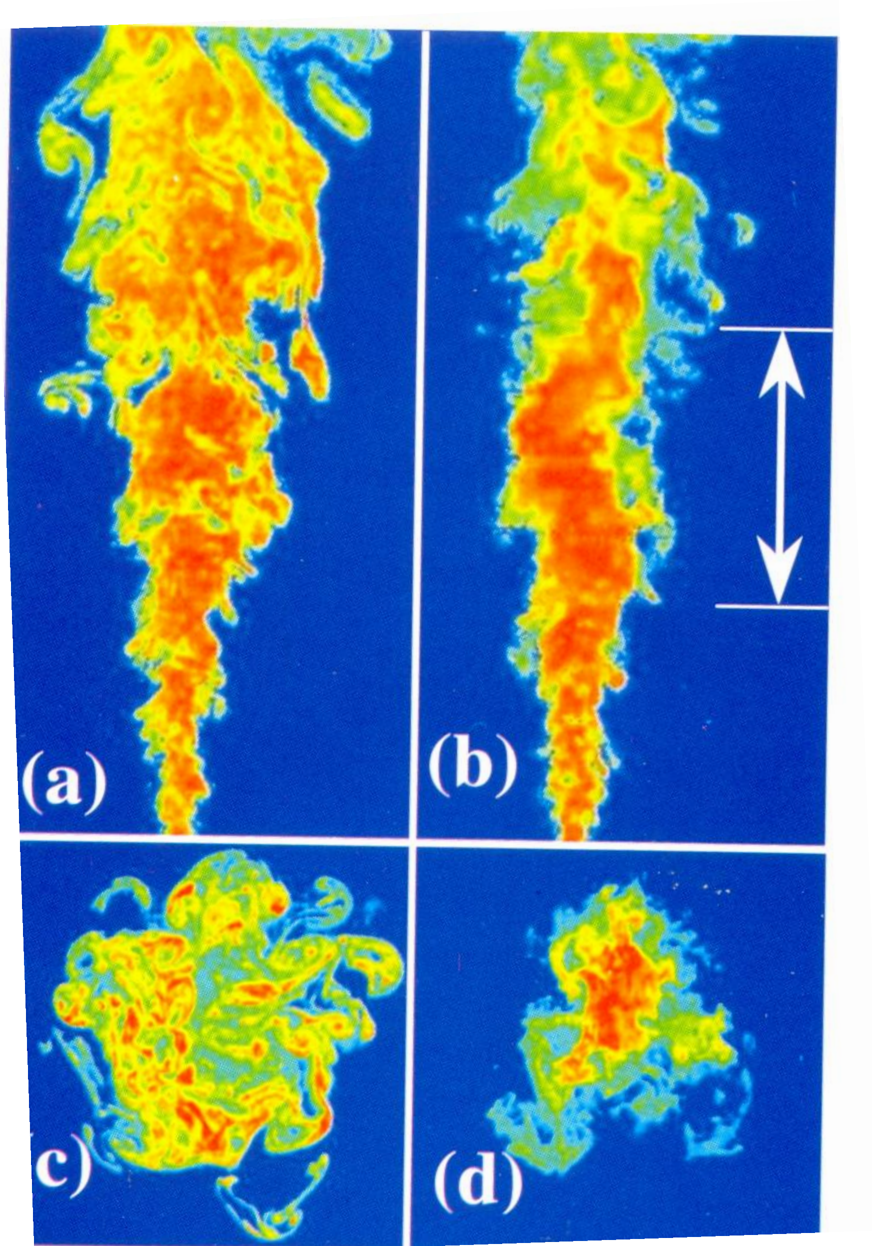

Left : No off-source heating
Right : Off-source heating over region shown

Based on Venkatakrishnan + 1998

TURBULENT ENTRAINMENT:
How Ambient becomes Cloud Fluid

Stage I: Engulfment – the induced action of large eddies in bringing the ambient non-turbulent air into the plume /jet

Stage II: Mingling – the stirring action of eddies in breaking down the large non-turbulent parcels into smaller and smaller scales

Stage III: Mixing – the action of molecular diffusion (t the scales) to make the mingled fluid turbulent i.e. to convert dry air into saturated cloudy air

Lehmann, Siebert and Shaw (2009): homogeneous versus inhomogeneous mixing

Brown, Roshko JFM

VARIATION OF ENTRAINMENT COEFFICIENT

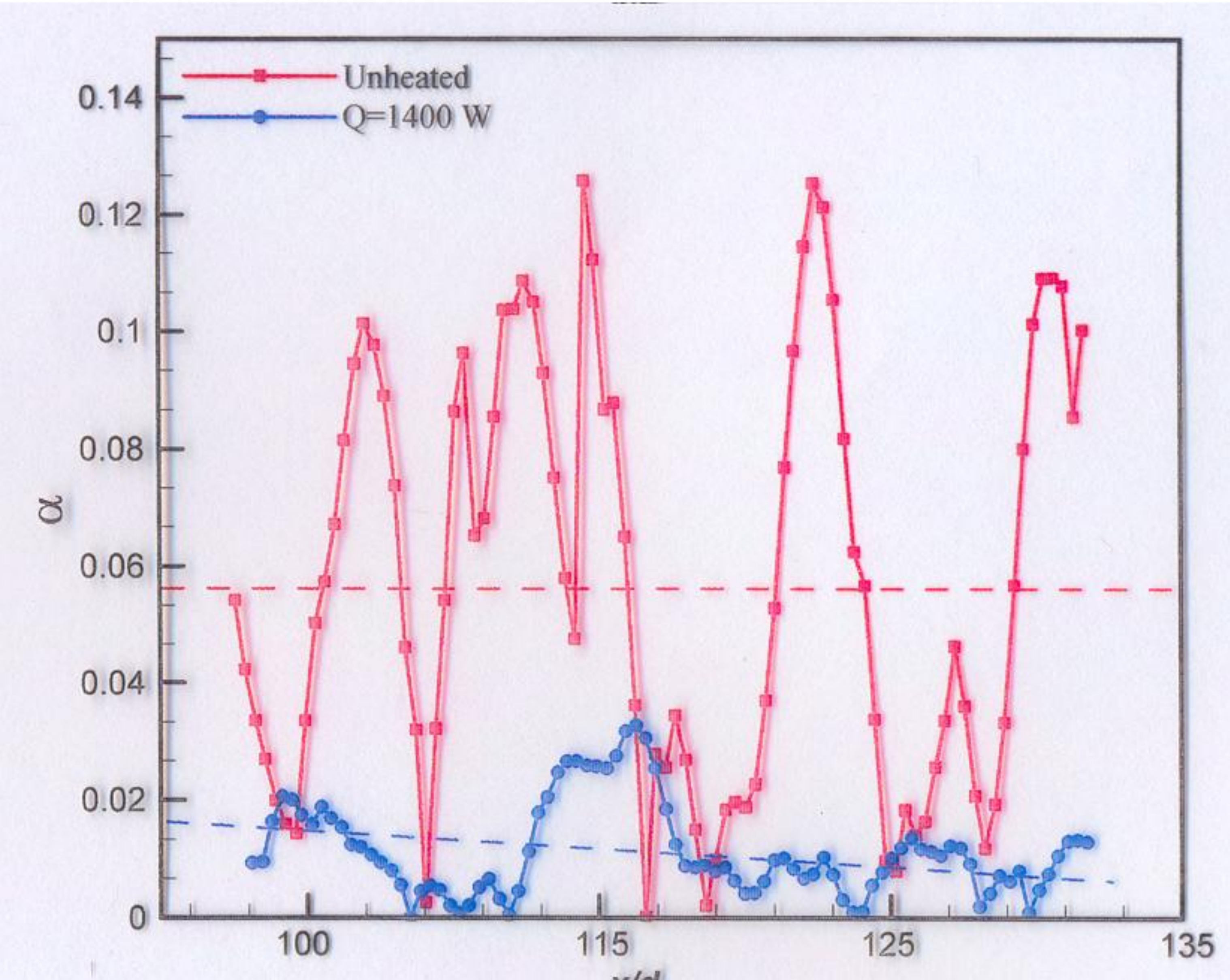

Variation of entrain-ment coefficient with axial distance Venkata-krishnan + 2003 *Curr. Sci.*

MEASURED ENTRAINMENT COEFFICIENTS, STEADY FLOWS

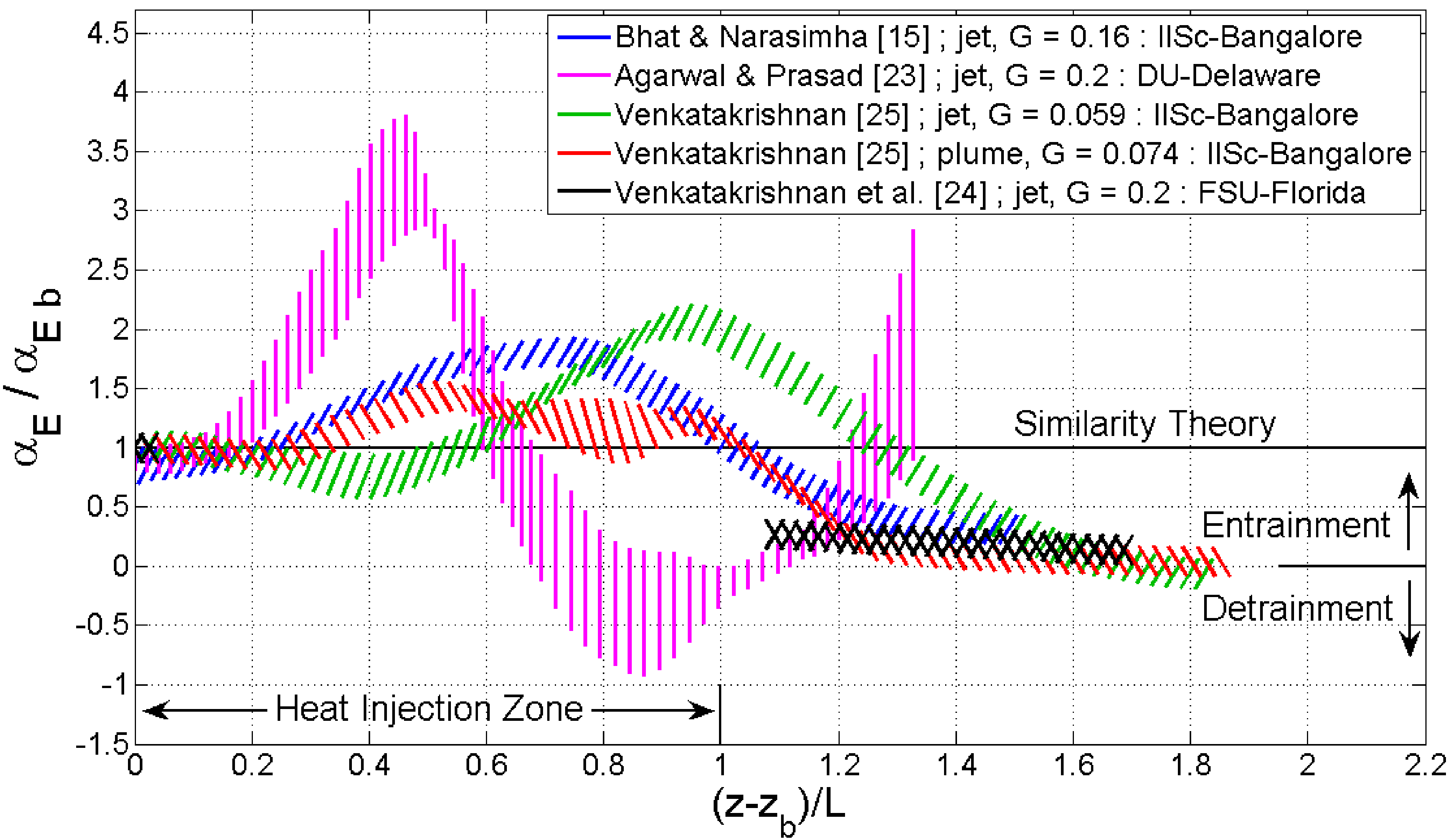

DILUTION AND PURITY

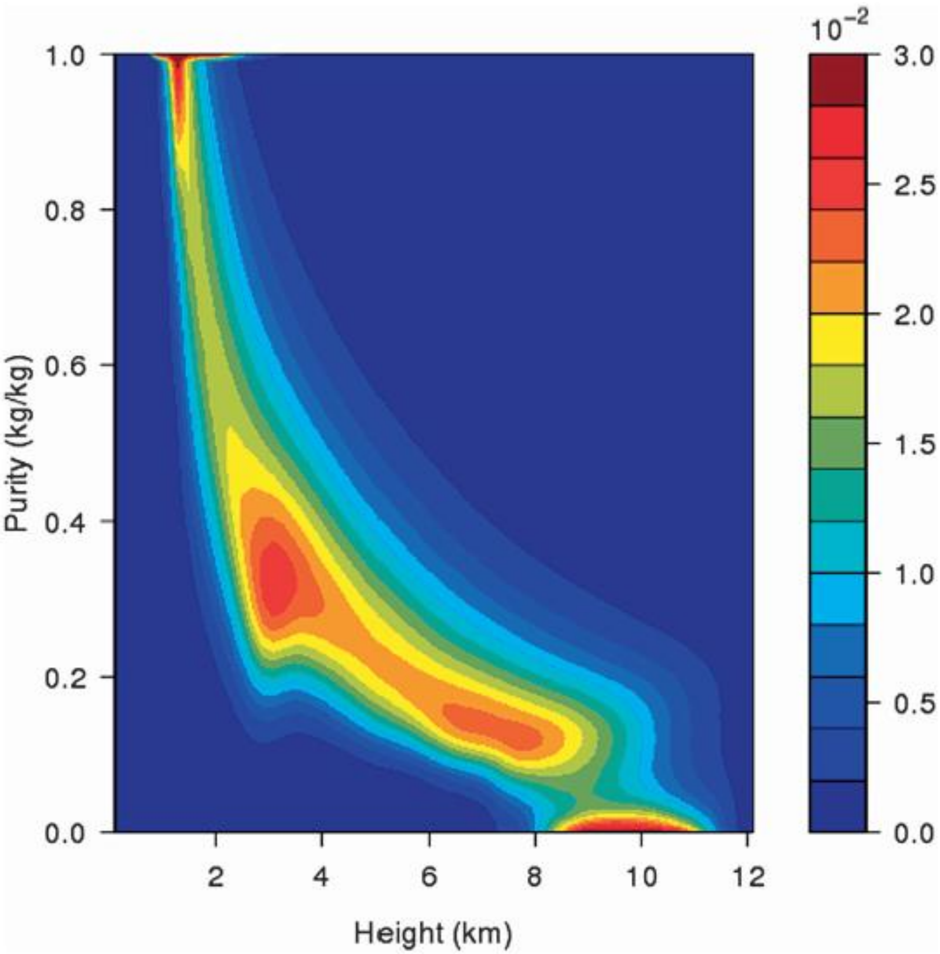

Romps & Kuang 2010 JAS

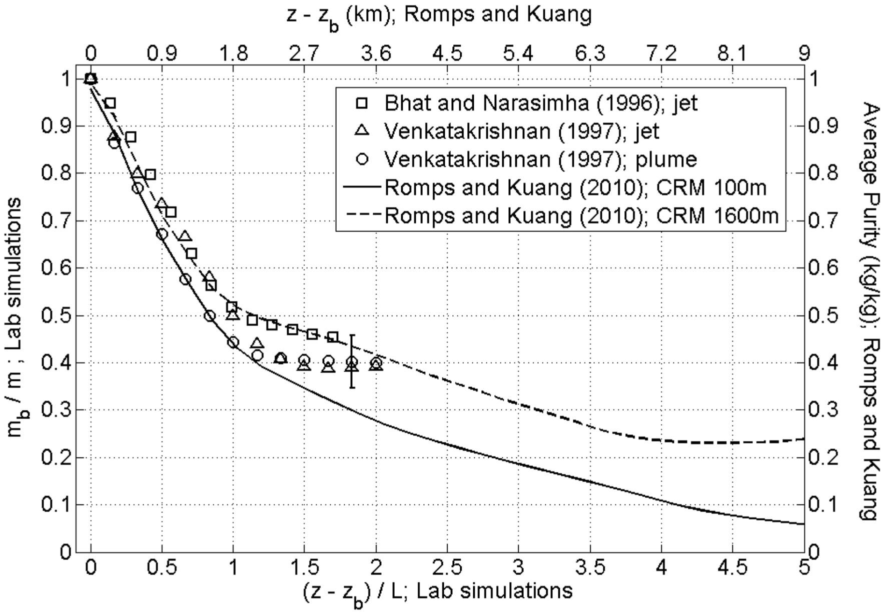

Comparison with Lab results
(RN+2011PNAS)

FIRST ORDER NON-PRECIPITATING CUMULUS SYSTEM

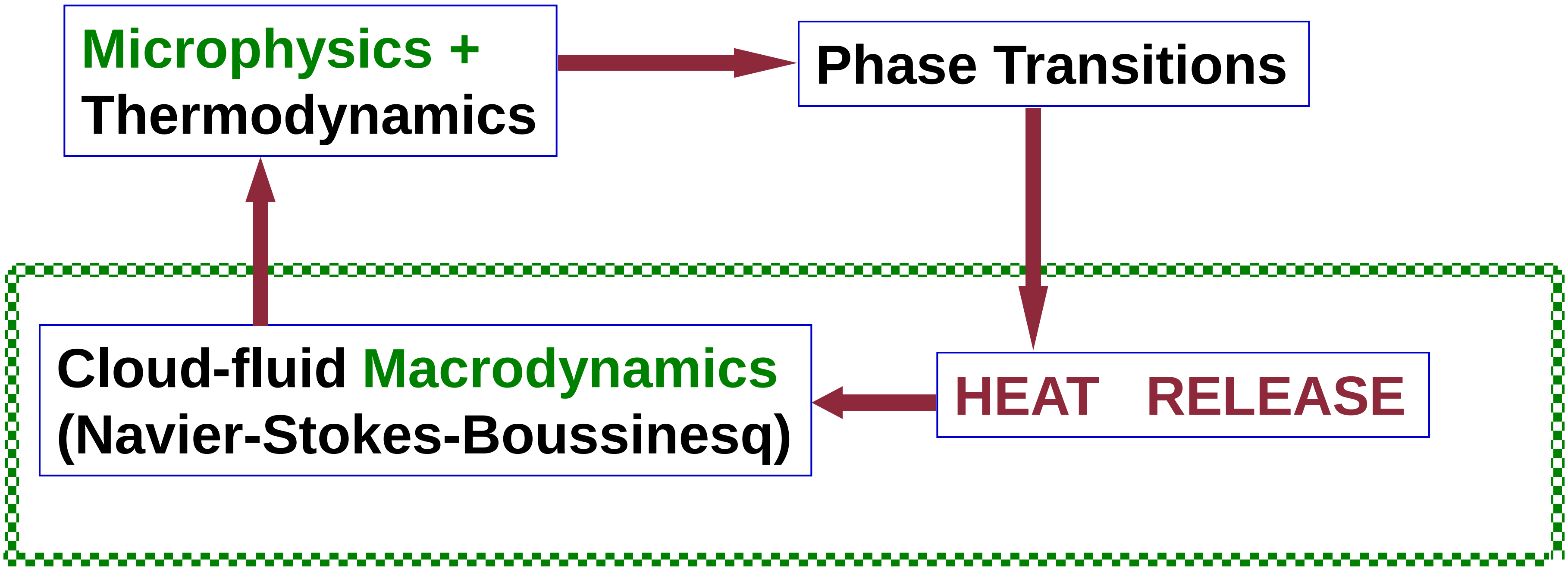

PARTING THOUGHT

Cumulus flows are

T R A N S I E N T   D I A B A T I C   P L U M E S

Particle Image Velocimetry (PIV)

Measuring area : 380X280 mm^2
LASER: ND-YAG pulse rate-10Hz, 200mJ/pulse, Pulse width 4ns
Camera: IDT-Y5 ,
Software: IDT ,Provision
Processing: Interrogation window = 32X32
Overlap = 50%
No. of vectors = 10K

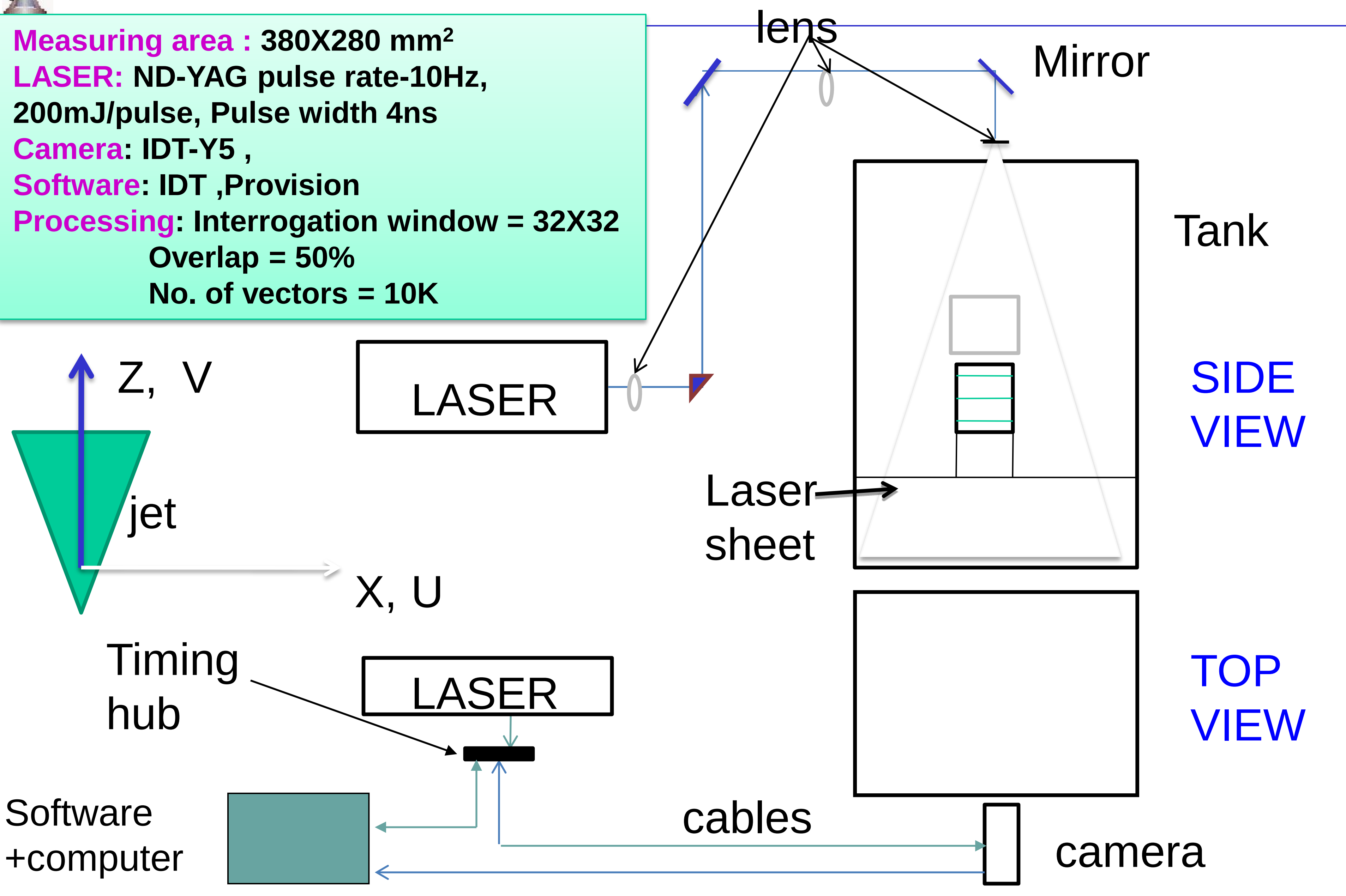

MEAN VELOCITY AND VORTICITY FIELDS

Stream-wise mean velocity

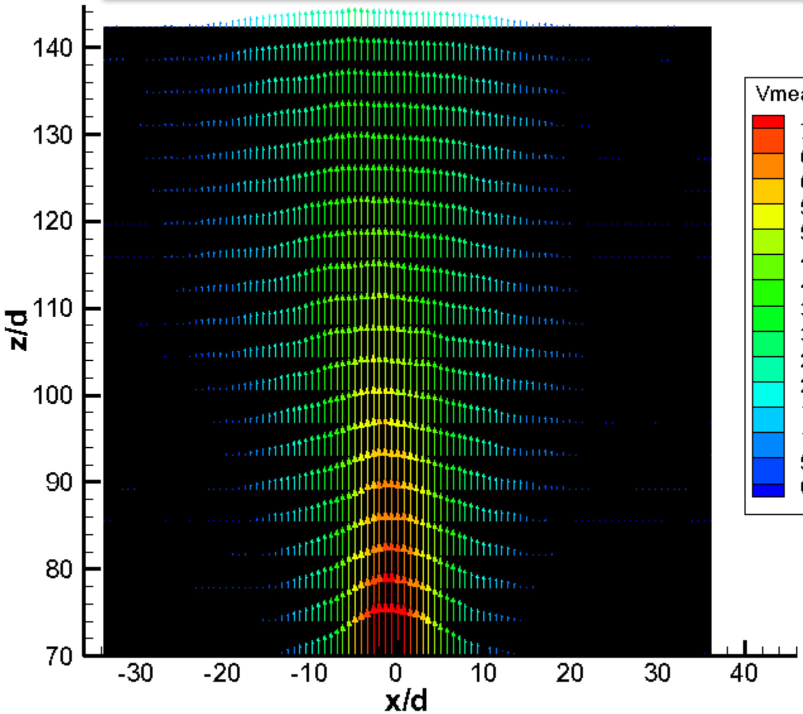

Mean vorticity (y component)

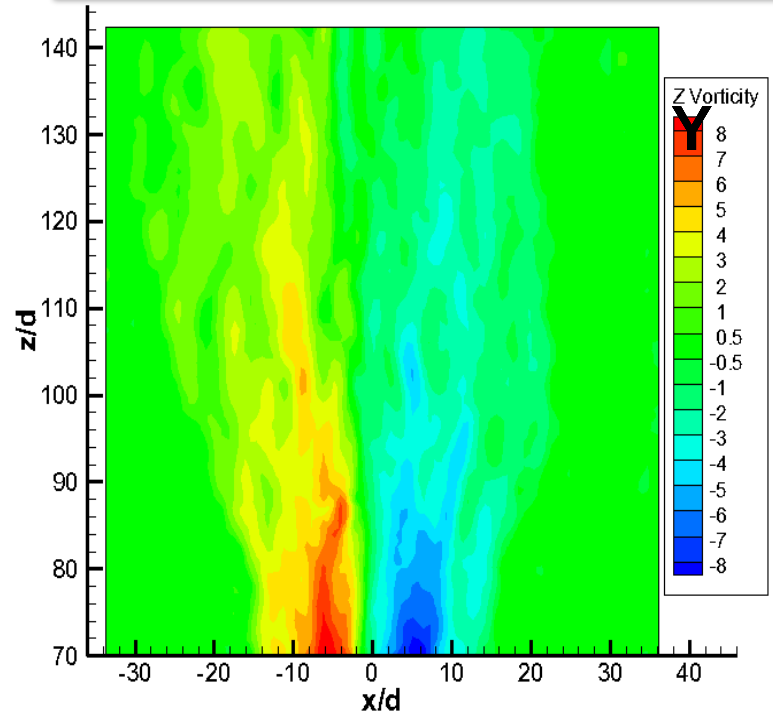

V_{exit} = 0.88 m/s , d = 4 mm , Re ~ 3500, G = 0, Experiment duration = 64s

Averaging time = 20 s

Vybhav + 2012 IITM Pune

Variation of mass flux with height

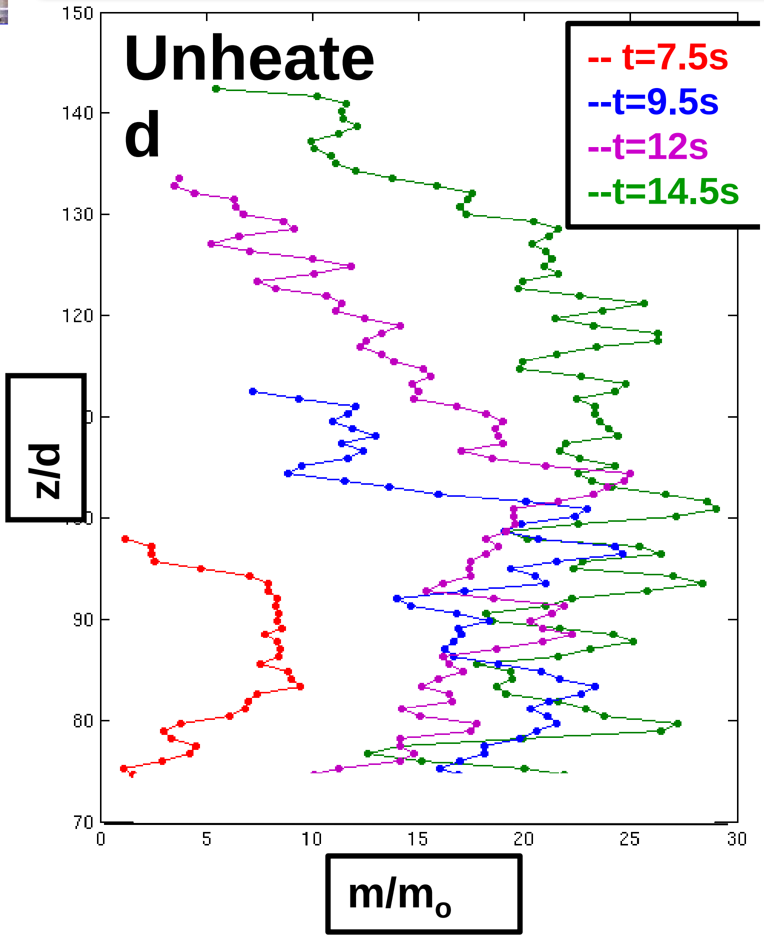

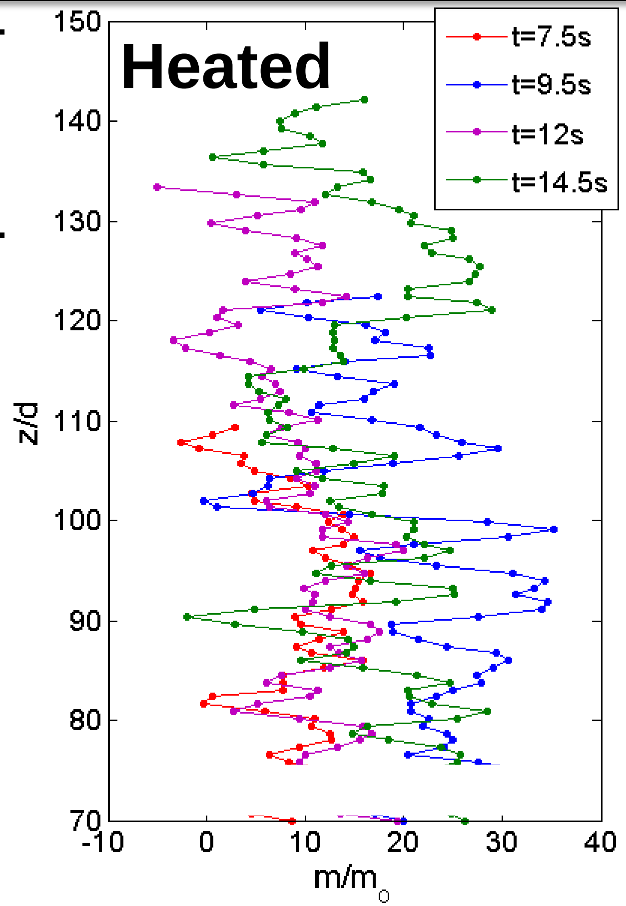

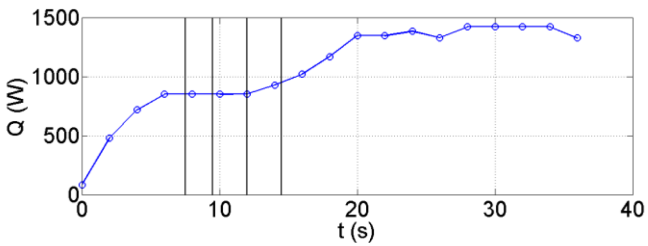

V_{exit} = 0.88 m/s , d = 4 mm, Re ~ 3500

Calculation of Entrainment Coefficient

Unheated Jet

$$\alpha_E = \frac{\frac{dm}{dz}}{2\pi\rho b_v V_c}$$

- Large statistical fluctuations observed that are inherent in instantaneous flow fields
- Data smoothing necessary

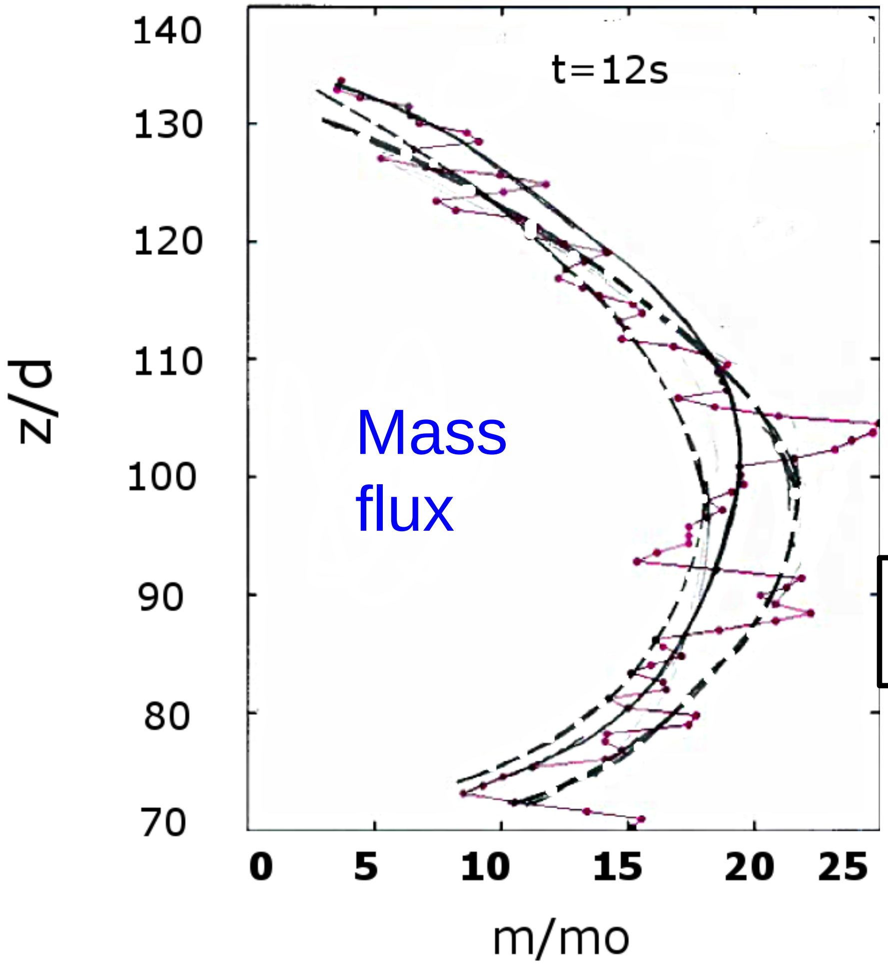

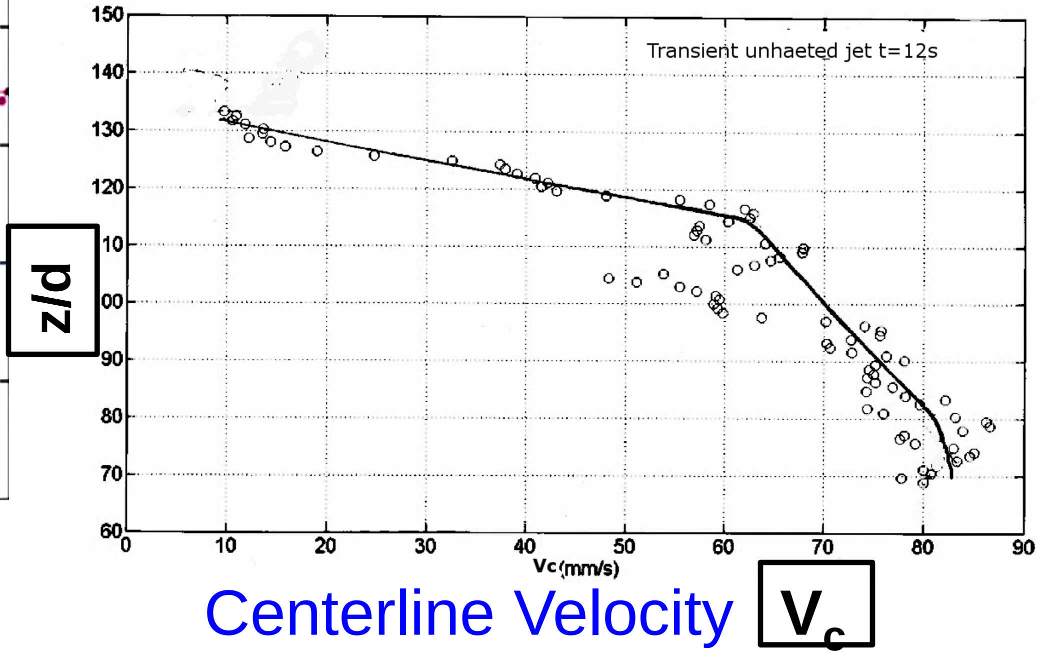

Effect of Heating on Entrainment Coefficient

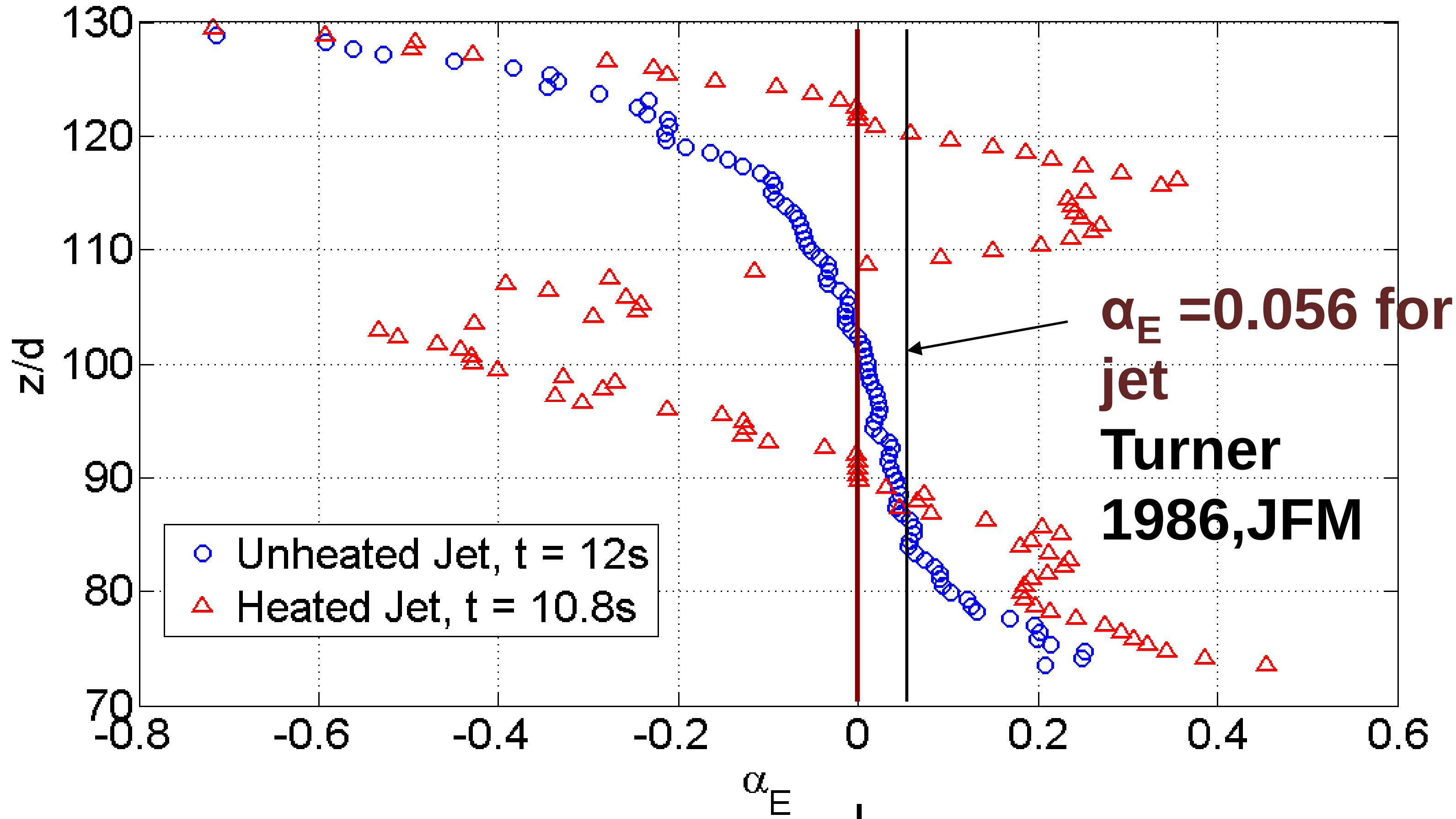

Detrainment-like behavior

Entrainment

V_{exit} = 0.875 m/s , d = 4 mm, Re ~ 3500, For heated jet Q ~ 850 W

Conclusions

1. We now have a laboratory apparatus that can simulate a complete life-cycle of an evolving cumulus cloud.
2. The capability of measuring entrainment co-efficient in a transient diabatic jet is demonstrated.
3. The large variation in entrainment coefficient values are because of the statistical fluctuations inherent in individual realizations. With averages taken over an ensemble of five to ten realizations, these fluctuations can be smoothed out (work in progress).
4. The present technique has the capability to provide precise entrainment data on cumulus cloud flows, and hence to help in devising better cumulus parameterization schemes.

THE GOAL, 2010

Real Cloud

Laboratory Cloud

Cyber Cloud

?

LABORATORY SETUP AND TEMPORAL SIMULATION OF STEADY JETS

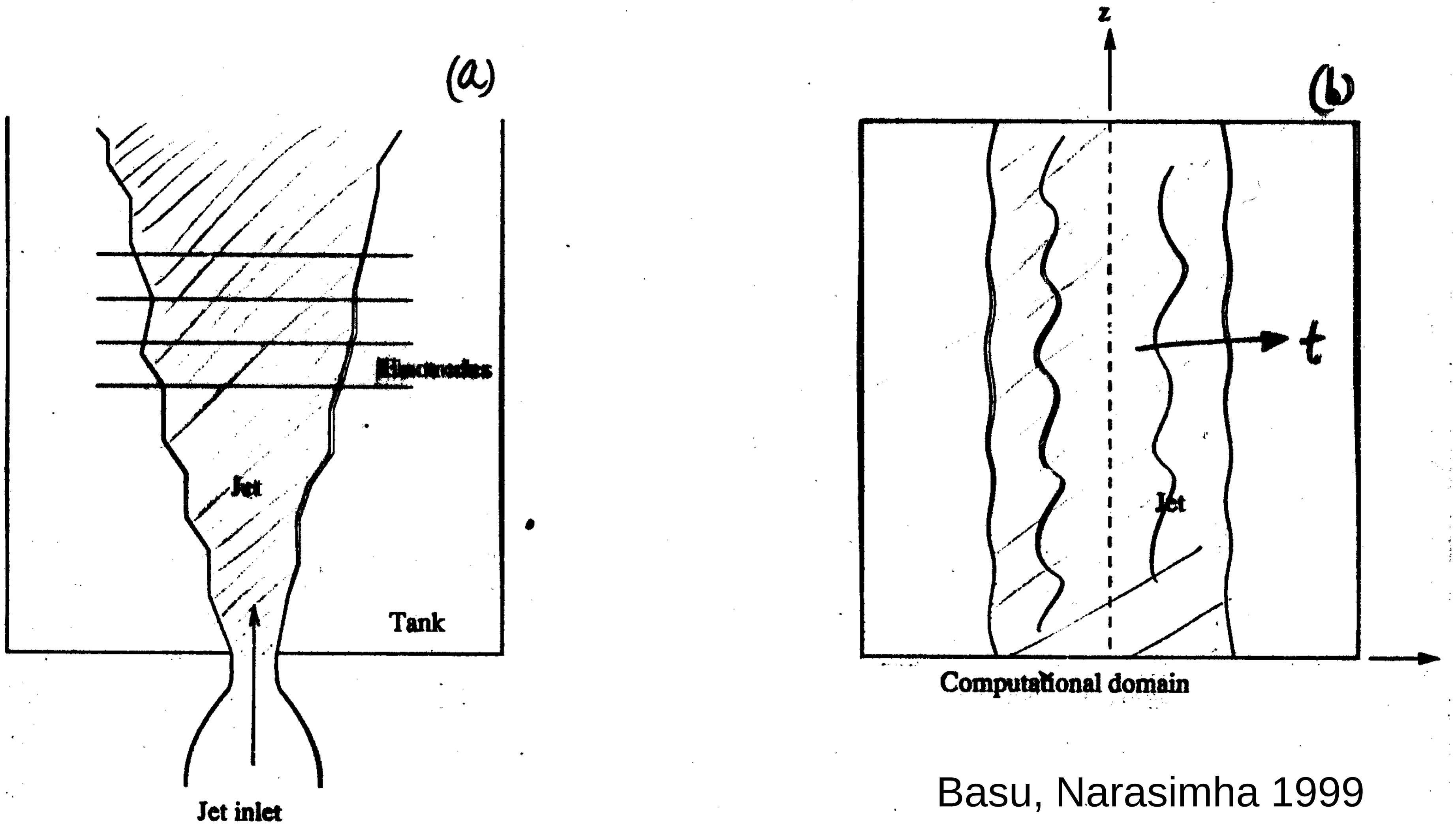

Basu, Narasimha 1999

EQUATIONS FOR A 'BOUSSINESQ CLOUD'

$$\nabla \cdot \boldsymbol{u} = 0,$$ (mass)

$$\frac{\partial \boldsymbol{u}}{\partial t} + (\boldsymbol{u} \cdot \nabla)\boldsymbol{u} = -\frac{1}{\rho}\nabla p + \nu \nabla^2 \boldsymbol{u} - \boldsymbol{g}\alpha T,$$ (momentum)

$$\frac{\partial T}{\partial t} + (\boldsymbol{u} \cdot \nabla) T = \kappa \nabla^2 T + \frac{J}{\rho\, c_p} \boldsymbol{H}$$ (energy)

Basu, RN 1999 *J. Fluid Mech.*

VORTICITY IN BOUSSINESQ CLOUD

$$\frac{\partial \boldsymbol{\omega}}{\partial t} + \underbrace{(\boldsymbol{u} \cdot \nabla)\boldsymbol{\omega}}_{\text{advect}} - \underbrace{(\boldsymbol{\omega} \cdot \nabla)\boldsymbol{u}}_{\text{tilt, stretch}} - \underbrace{\nu \nabla^2 \boldsymbol{\omega}}_{\text{diffuse}} = \underbrace{\alpha \boldsymbol{g} \times \nabla T}_{\text{create}}$$

$$\left.\begin{aligned} \boldsymbol{u}(\boldsymbol{x},t) &= \boldsymbol{u}(\boldsymbol{x}+L\mathbf{e}_i,t), \quad & p(\boldsymbol{x},t) &= p(\boldsymbol{x}+L\mathbf{e}_i,t), \\ T(\boldsymbol{x},t) &= T(\boldsymbol{x}+L\mathbf{e}_i,t), & i &= 1,2,3. \end{aligned}\right\}$$

Basu, RN 1999 *J. Fluid Mech.*

THE BOUSSINESQ CLOUD EQUATIONS

$$\boldsymbol{u}(\boldsymbol{x},t)=\sum_{k'\leqslant K}\hat{\boldsymbol{u}}(\boldsymbol{k}',t)\exp\left(\mathrm{i}\frac{2\pi}{L}\boldsymbol{k}'\cdot\boldsymbol{x}\right)$$

$$\mathrm{i}\boldsymbol{k}\cdot\hat{\boldsymbol{u}}=0,$$

$$\frac{\partial\hat{\boldsymbol{u}}}{\partial t}=-[(\boldsymbol{u}(\boldsymbol{x},t)\cdot\nabla)\boldsymbol{u}(\boldsymbol{x},t)]_{\boldsymbol{k}}-\mathrm{i}\boldsymbol{k}\hat{p}-\frac{1}{Re}k^2\hat{\boldsymbol{u}}+H'(t)G^*\hat{T}\boldsymbol{e}_z,$$

$$\frac{\partial\hat{T}}{\partial t}=-[(\boldsymbol{u}(\boldsymbol{x},t)\cdot\nabla)T(\boldsymbol{x},t)]_{\boldsymbol{k}}-\frac{1}{Re\,Pr}k^2\hat{T}+H(t)\frac{d_0}{U_0t_h}\hat{g}(r),$$

THE BOUSSINESQ CLOUD EQUATIONS

Using continuity, can eliminate pressure and replace first two terms on r.h.s. of momentum equation by

$$-\frac{\mathrm{i}}{2} Q_{\alpha\beta\gamma}(\boldsymbol{k}) \sum_{\substack{\boldsymbol{m}+\boldsymbol{n}=\boldsymbol{k} \\ m,n \leqslant k}} u_\beta(\boldsymbol{m}, t) u_\gamma(\boldsymbol{n}, t),$$

where

$$Q_{\alpha\beta\gamma} = k_\beta(\delta_{\alpha\gamma} - k_\alpha k_\gamma / k^2) + k_\gamma(\delta_{\alpha\beta} - k_\alpha k_\beta / k^2).$$

CREATING VORTICITY BY BAROCLINIC TORQUE

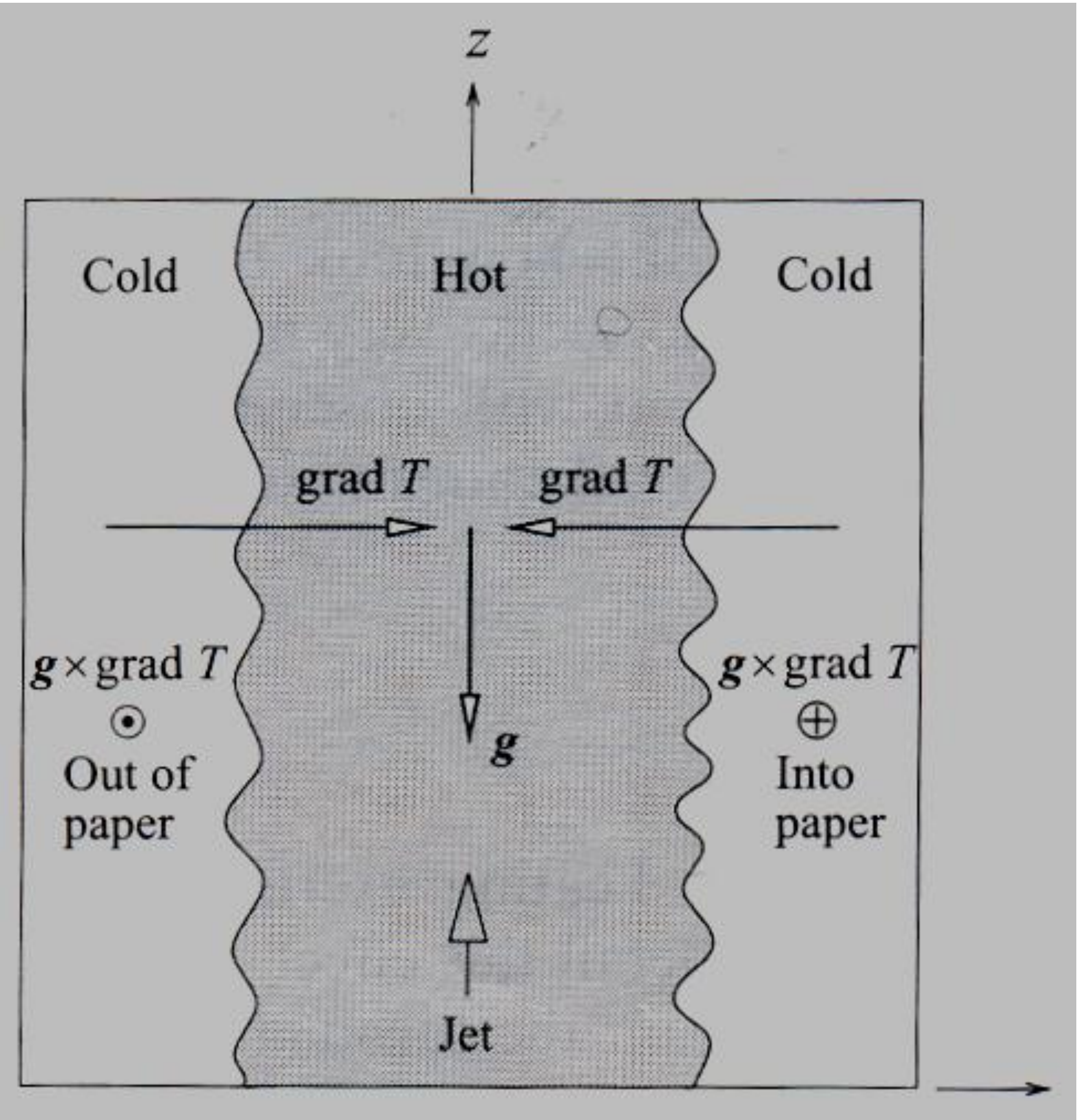

Basu, RN 1999 *J. Fluid Mech.*

COHRERENT STRUCTURE IN AZIMUTHAL VORTICITY

UNHEATED JET

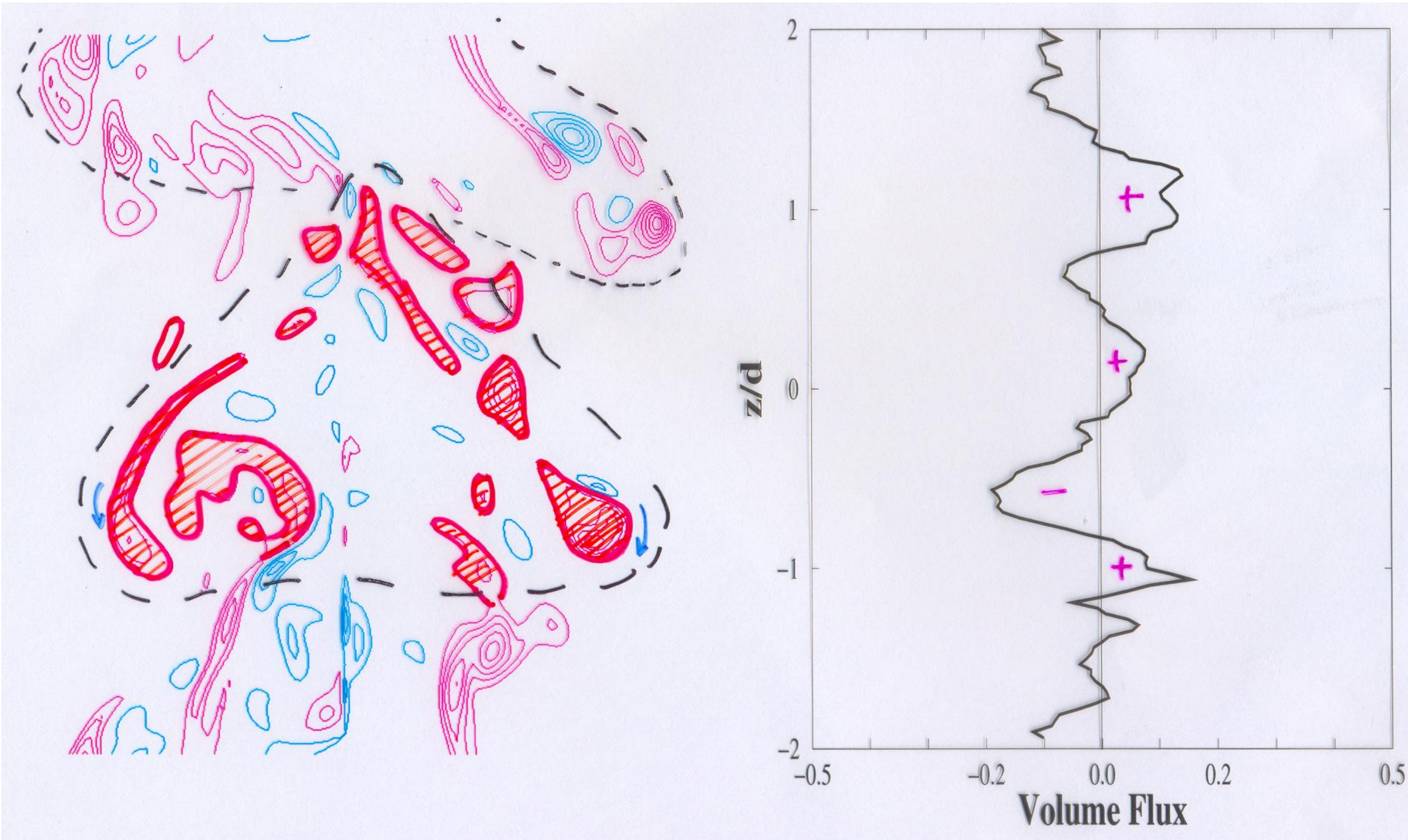

t = 35, x = 65

Volume flux vs. z/d at t = 35

RN, Shivakumar 1999 IUTAM Goettingen

AZIMUTHAL VORTICITY
FULLY HEATED JET

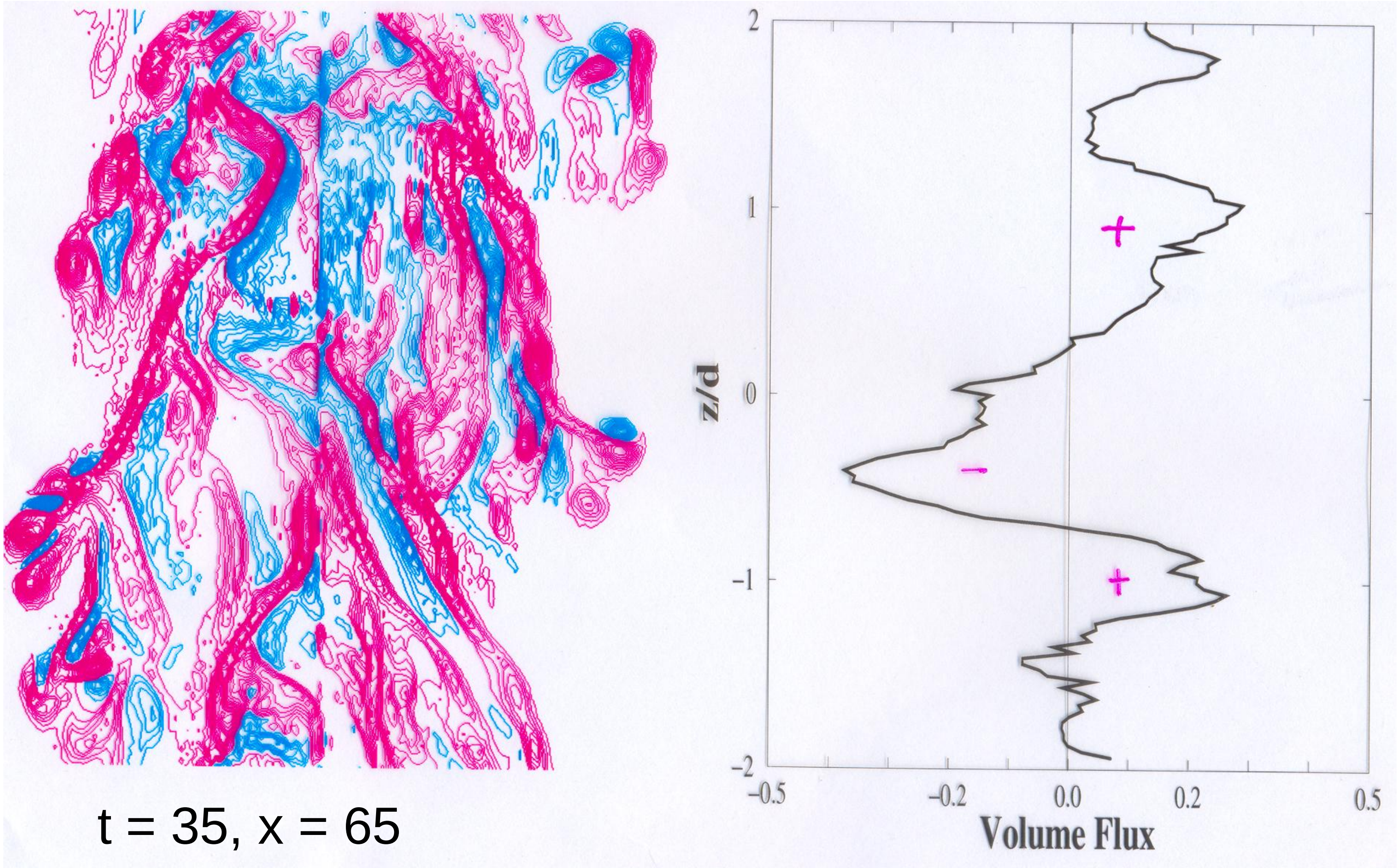

RN, Shivakumar 1999 IUTAM Goettingen

Volume flux vs. z/d at t = 35

UNHEATED, HEATED JETS

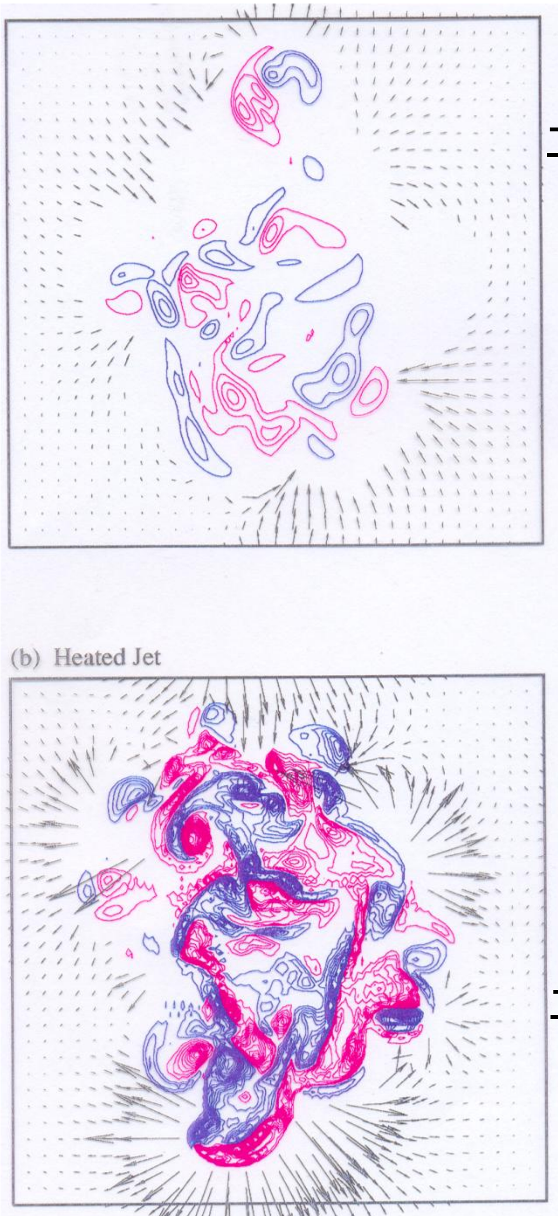

$\pm\ \omega_z$: 0.2(0.2)3

Section at Widest Station

$\pm\ \omega_z$: 0.5(0.5)10

(Confirmed by Sau 2011 *Phys. Fluids*)

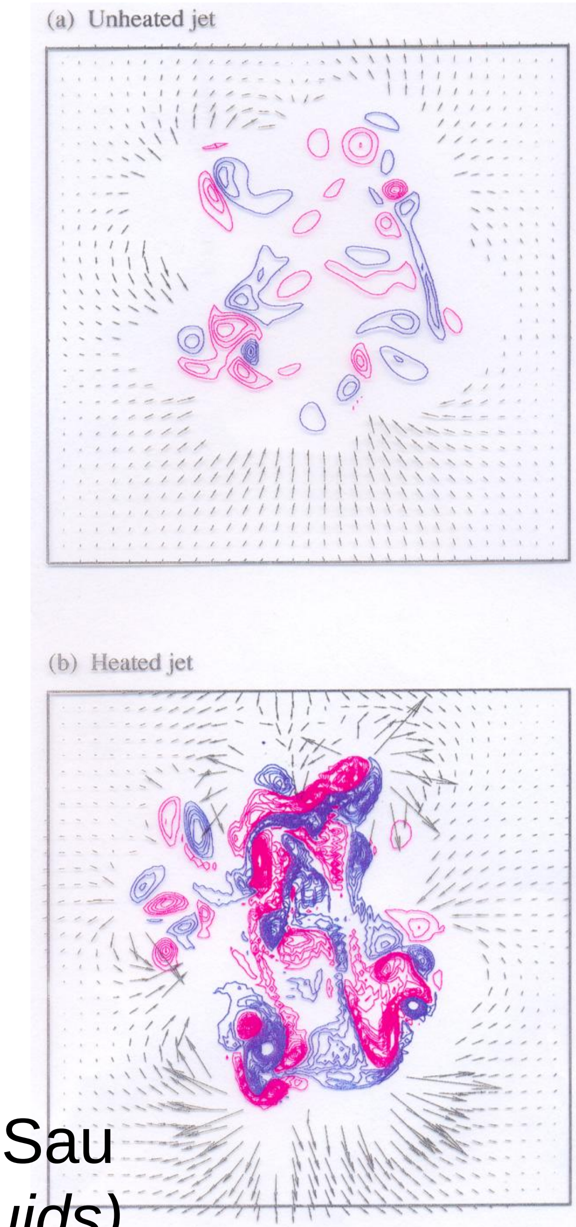

Section at Narrowest Station

RN, Bhat 2008

HOW VORTICITY GOES FROM 1D TO 3D

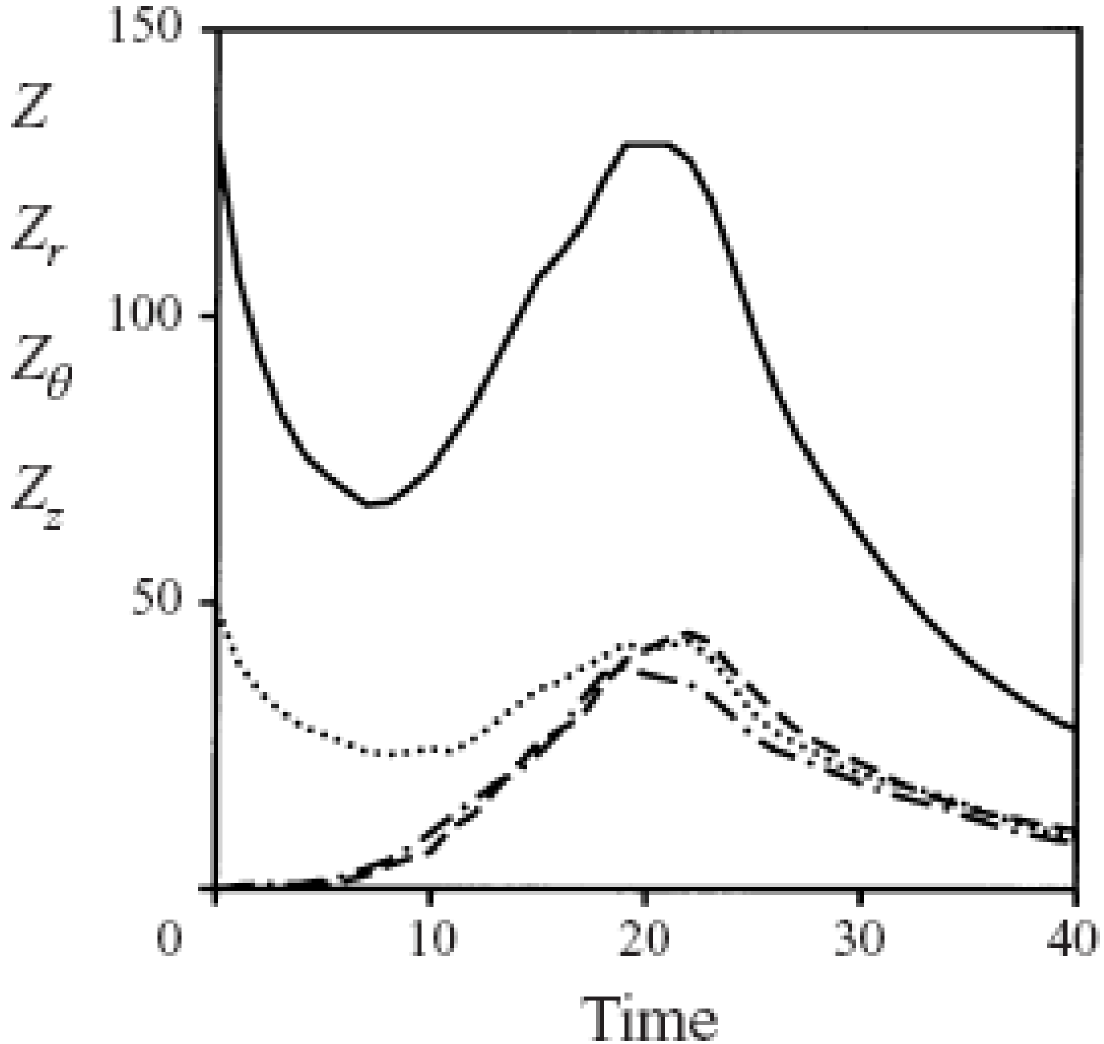

Enstrophy Z = mean square vorticity

Computed evolution of enstrophy in the unheated jet
From the top: total, azymuthal, axial, radial. Basu, RN 1999 *JFM*

VORTICITY SPECTRA

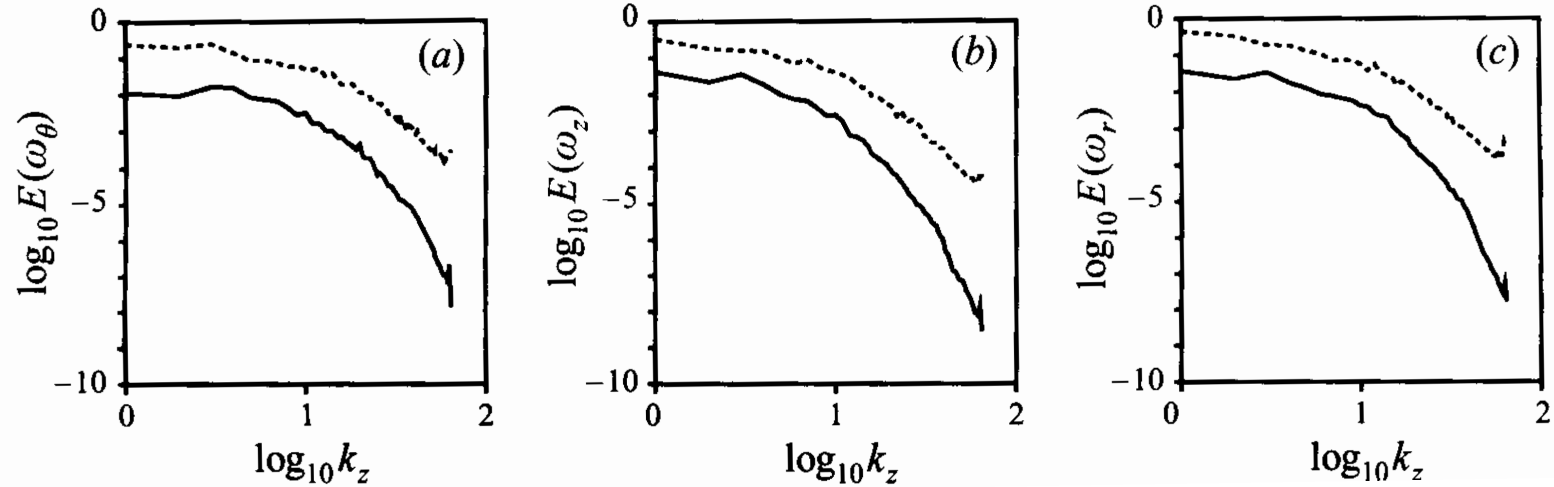

Effect of diabatic heating on spectra of different components of vorticity (from left azimuthal, axial and radial). Heated (upper curve) and unheated (lower curve). Note that heating enhances high wave number spectra by a factor of nearly 10^4.

COMPUTATION OF

TRANSIENT DIABATIC PLUMES

Prasanth, Deshpande, RN, 2013

WHERE WE ARE, 2013

Real Cloud

NOAA Research, Jim Lee

Laboratory Cloud

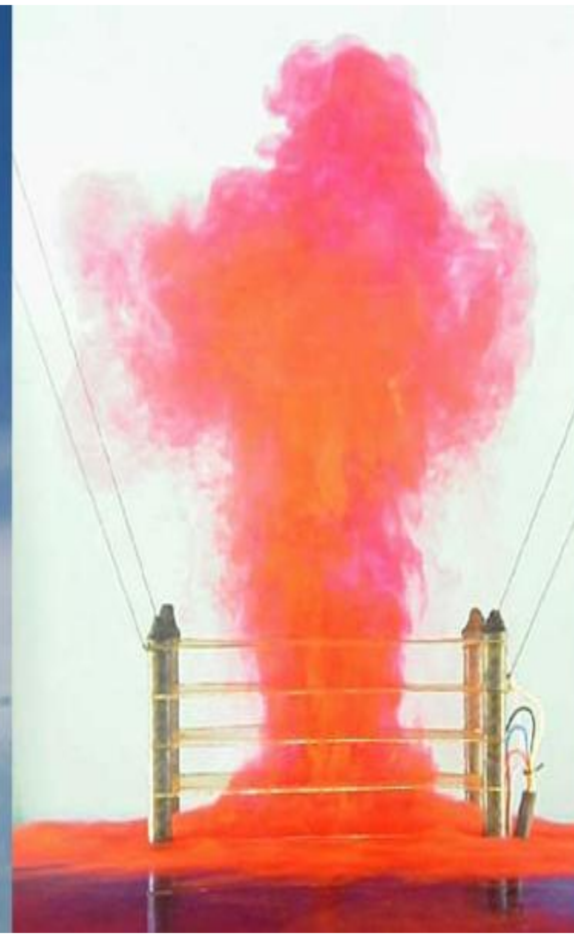

RN ++ 2011 *PNAS*

Cyber Cloud

Present Simulation

NAVIER-STOKES-BOUSSINESQ

$$\nabla.\mathbf{u} = 0, \quad \text{(mass)}, \tag{4}$$

$$\frac{\partial \mathbf{u}}{\partial t} + (\mathbf{u}.\nabla)\mathbf{u} = \frac{1}{\rho_o}\nabla p + \nu\nabla^2\mathbf{u} - \mathbf{g}\beta T \quad \text{(momentum)}, \tag{5}$$

$$\frac{\partial T}{\partial t} + (\mathbf{u}.\nabla)T = \kappa\nabla^2 T + \frac{J}{\rho_0 c_p} \quad \text{(energy)}, \tag{6}$$

$$\frac{\partial c}{\partial t} + (\boldsymbol{u}.\nabla)c = \kappa_d \nabla^2 c \quad \text{(passive scalar)},$$

$$\frac{\partial \omega}{\partial t} + (\mathbf{u}.\nabla\omega) - (\omega.\nabla)\mathbf{u} - \nu\nabla^2\omega = \beta\mathbf{g} \times \nabla T \quad \text{(vorticity)}. \tag{7}$$

THE SOLVER

- Discretely kinetic energy preserving scheme (in the inviscid limit)
- Staggered-clustered grid
- Second order Adams-Bashforth time-integration scheme
- Poisson Solver:
  - Successively over-relaxed Gauss-Seidel (optimized by Intel, Bangalore).
  - Multigrid based.

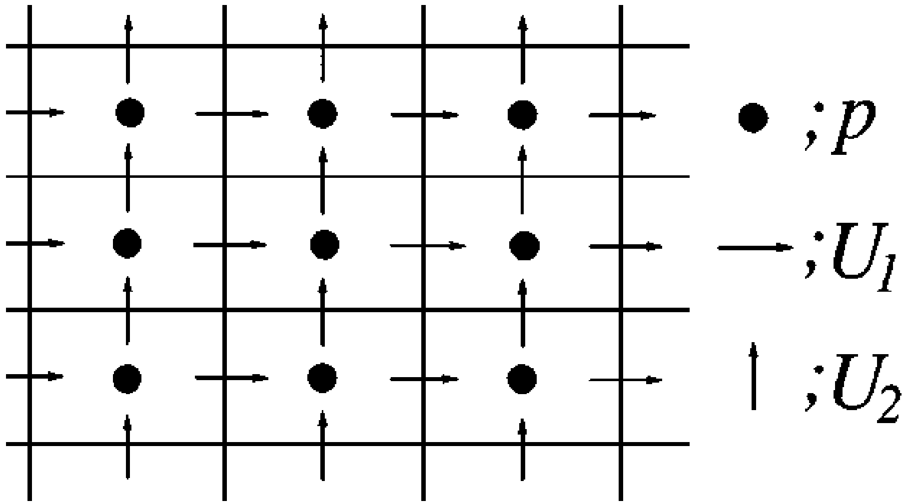

Staggered grid

Sample grid layout

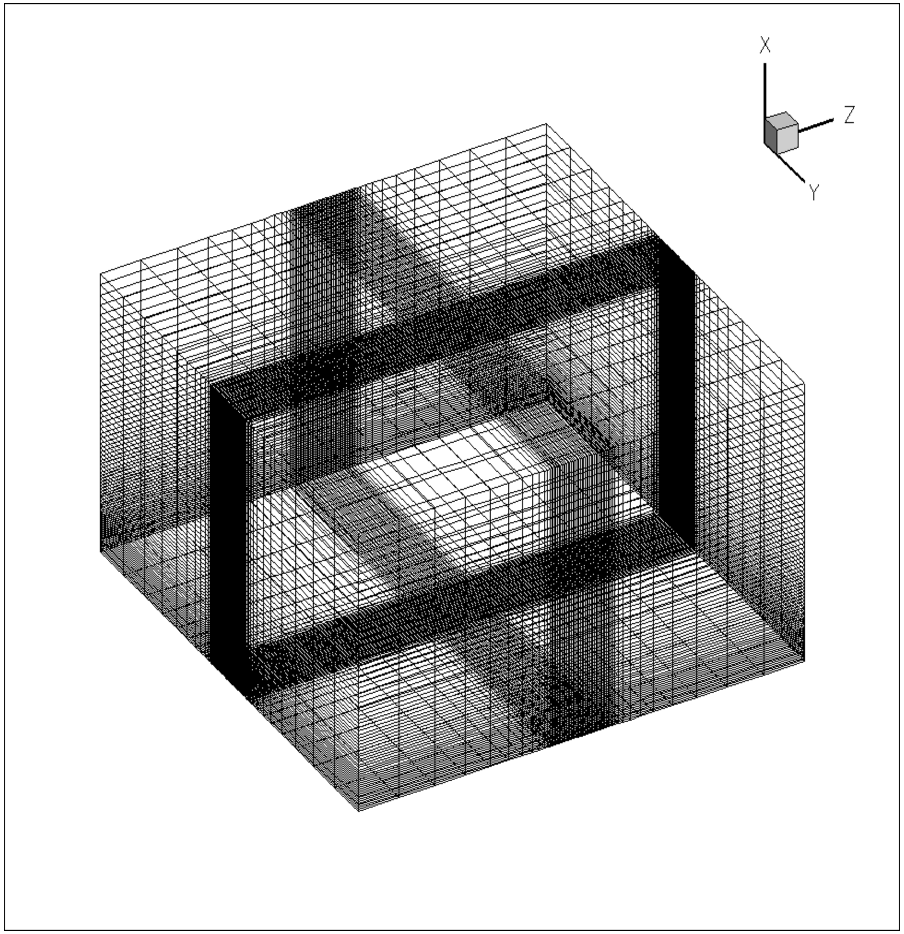

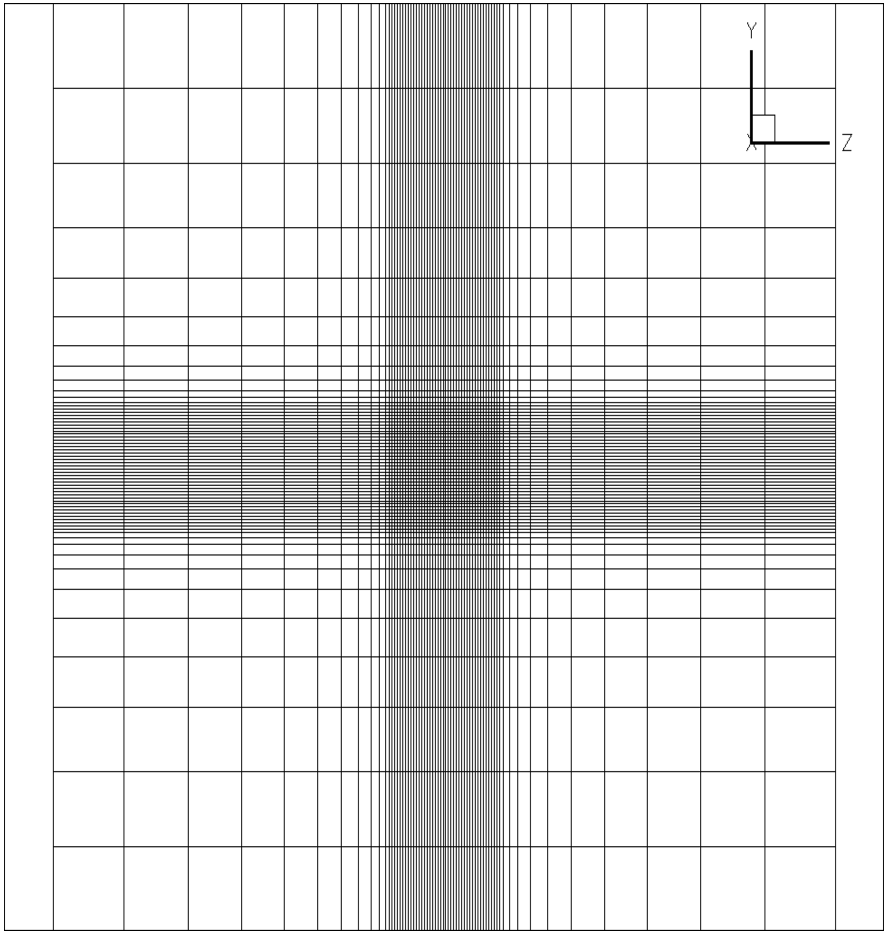

Grid Resolution

- Present coarse grid simulations
  - Grid: 4 million
  - RAM: 6.4 GB
  - HD Space: ~200 GB
  - Compute time on 64 proc: ~ 4 days
- Estimate for the final simulations
  - Grid : ~ 4 billion
  - RAM: ~ 7TB
  - HD Space: ~200 TB
  - Compute time: Depends on the scalability of the code

THE SOLVER

- Computing effort for N grid points :
  - Gauss Seidel based Solver ($O(N^{3/2})$)
  - Multigrid based Solver ($O(N)$)

These estimates may change depending on boundary conditions and grid (for example clustering factor)

Boundary conditions

- Bottom boundary: No slip wall with a buoyancy source.
- Lateral boundary: No slip adiabatic wall (similar to lab experiments).
- Top out flow: Zero normal derivative for all variables except pressure.

GAMES WITH CLOUDS : SOME STILLS

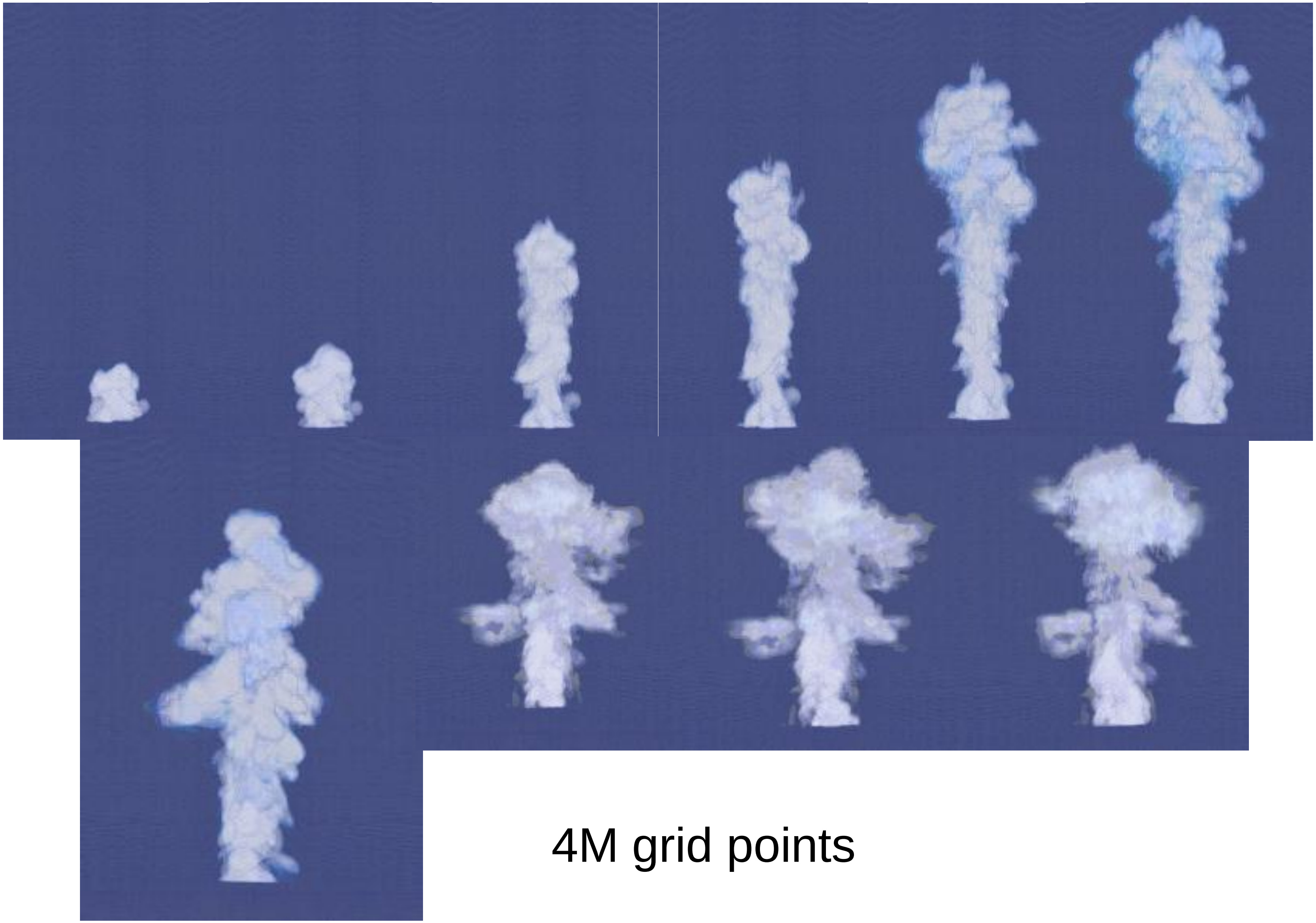

4M grid points

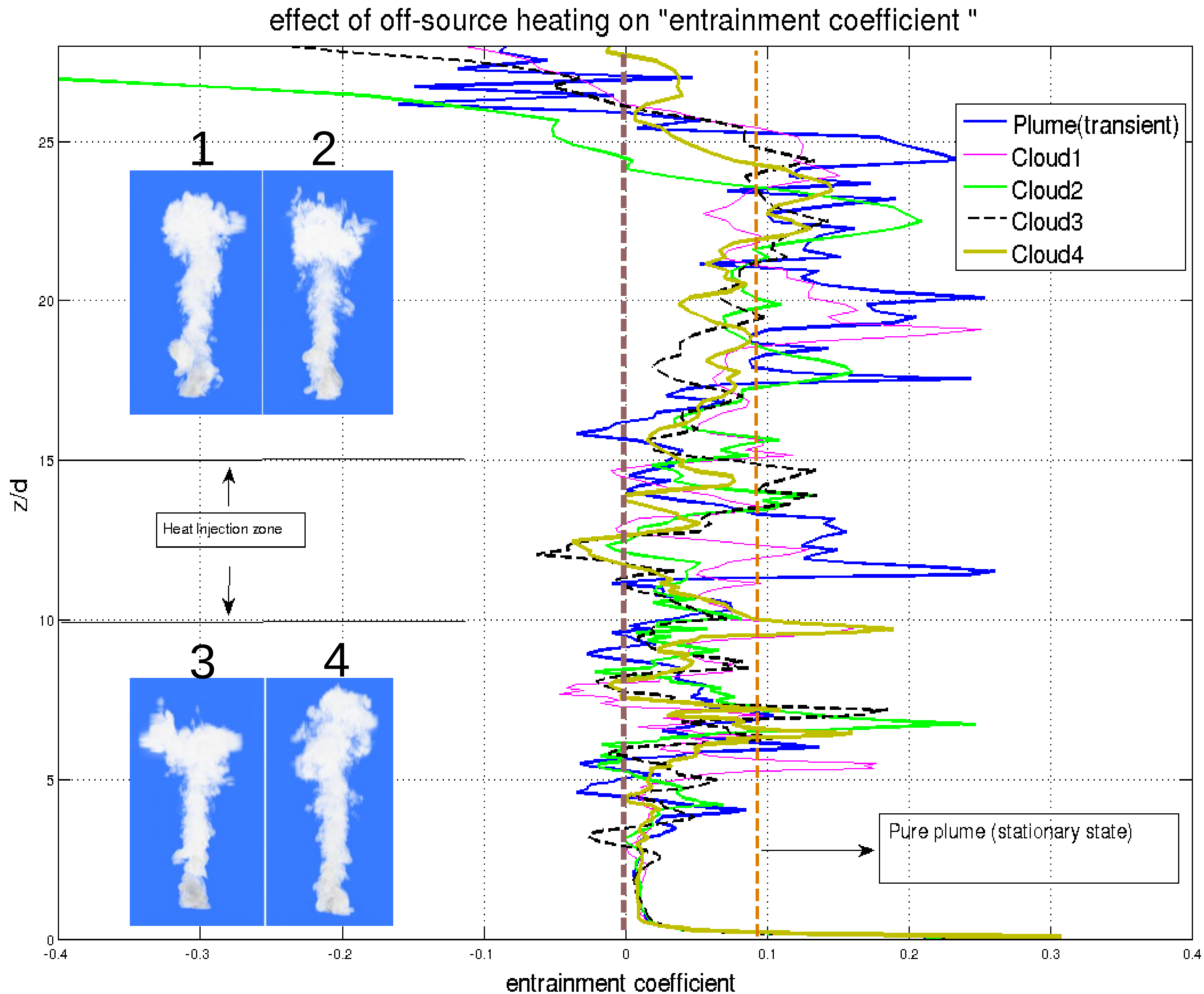

effect of off-source heating on "entrainment coefficient "
Plume(transient)
Cloud1
Cloud2
Cloud3
Cloud4
1
2
3
4
Heat Injection zone
Pure plume (stationary state)
z/d
entrainment coefficient
0
5
10
15
20
25
-0.4
-0.3
-0.2
-0.1
0
0.1
0.2
0.3
0.4

Vorticity component normal to the plane

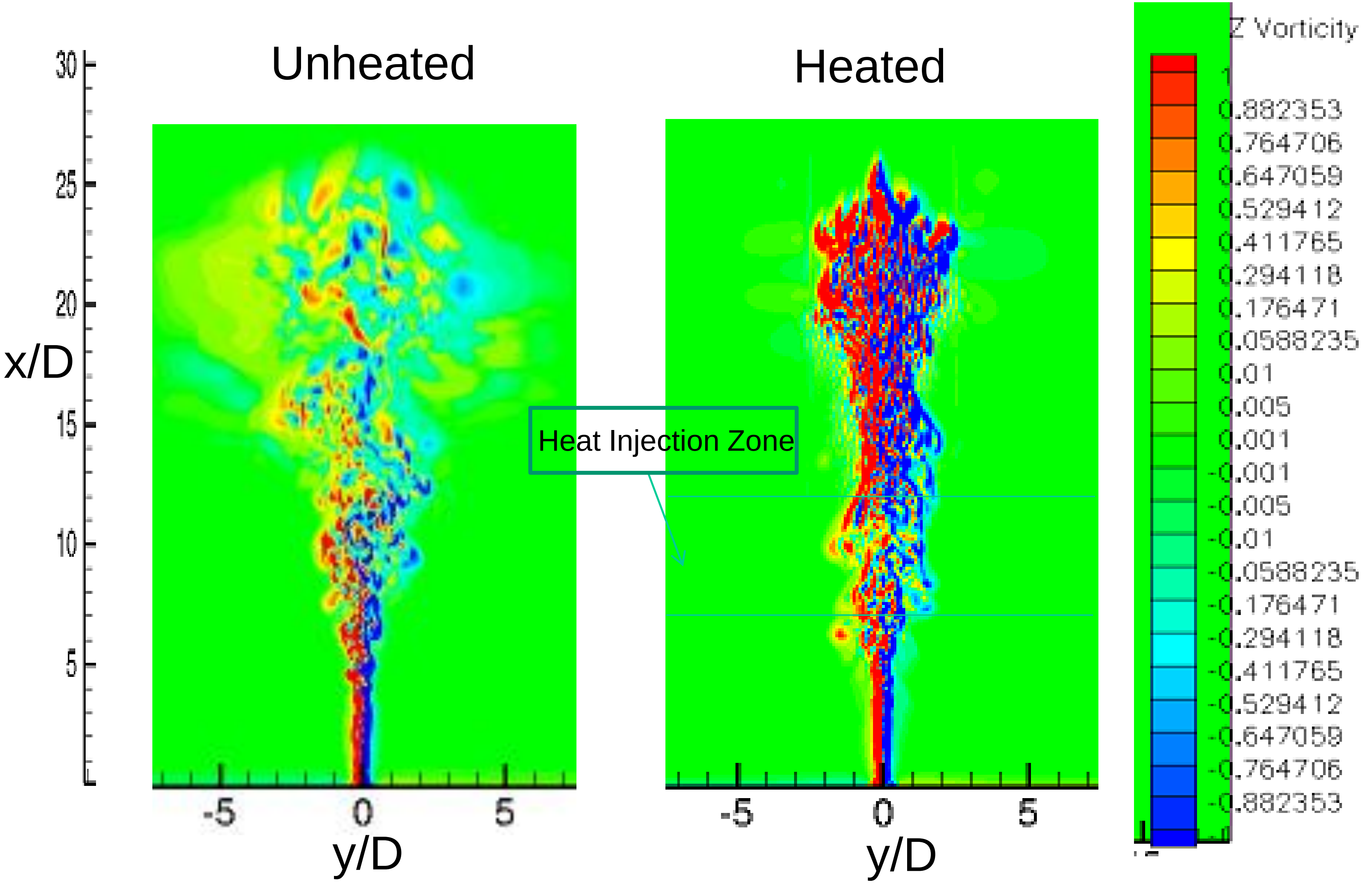

VORTICITY BUDGET

- For simplicity, consider a temporal diabatic jet/plume (Basu, RN 1999)
- Notation:

	Mean	Fluctuations	Rms
Velocity	***U***	***u'***	$\hat{u}$
Vorticity	$\boldsymbol{\Omega}$	$\boldsymbol{\omega}'$	$\hat{\omega}$
Temperature	$\overline{T}$	T'	$\hat{T}$
Strain rate	S_{ij}	s'_{ij}	

Vorticity budget continued…..

- Navier-Stokes + Mean Vorticity

$$\frac{\partial \Omega_i}{\partial t} = -\overline{u'_j \frac{\partial \omega'_i}{\partial x_j}} \text{ \{turbulent transport of turbulent vorticity\}}$$

$$+ \Omega_j S_{ij} \quad \text{\{mean flow stretching mean vorticity\}}$$

$$+ \overline{\omega'_j s'_{ij}} \text{ \{turbulent flow stretching turbulent vorticity\}}$$

$$+ \nu \frac{\partial}{\partial x_j} \frac{\partial \Omega_i}{\partial x_j} \text{ \{viscous diffusion\}} \quad \text{--------------->} \quad (1)$$

RN 2012 *JoT*

Vorticity budget continued…..

- Turbulent enstrophy:

$$\frac{\partial}{\partial t}\left(\frac{\hat{\omega}^2}{2}\right) = -\,\overline{u'_j\omega'_i}\,\frac{\partial \Omega_i}{\partial x_j}$$ {generation by mean vorticity gradient}

$$+\frac{\partial}{\partial x_j}\left(\frac{\overline{\omega'^2 u'_j}}{2}\right)$$ {turbulent transport}

$$+\ \overline{\omega'_i\omega'_j}S_{ij}$$ {stretching by mean strain}

$$+\,\overline{\omega'_i\omega'_j s_{ij}}$$ {stretching by turbulent strain}--- *

$$+\,\nu\frac{\partial}{\partial x_j}\frac{\partial}{\partial x_j}\left(\frac{\hat{\omega}^2}{2}\right)$$ {viscous diffusion}

$$-\ \nu\overline{\left(\frac{\partial \omega_i}{\partial x_j}\frac{\partial \omega_i}{\partial x_j}\right)}$$ {viscous dissipation} ---------------- * →(2)

Vorticity budget continued…..

Noting: $\Omega \sim S \sim \frac{U_c}{b}$, $\widehat{\omega} \sim s \sim \frac{\widehat{u}}{\lambda} \sim \Omega\, Re^{\frac{1}{2}}$, $\hat{u} \sim U_c$, Re = $\frac{U_c b}{\nu}$,

introducing Kolmogorov: $l_k = (\frac{\nu^3}{\varepsilon})^{\frac{1}{4}}$, $u_k \sim \frac{\nu}{k}$ and taking

$\frac{\partial \omega_i}{\partial x_j} \sim \frac{\widehat{u}'}{\lambda} \cdot \frac{1}{l_k}$,

we have enstrophy dissipation ~ $\nu \frac{\widehat{u}^3}{\lambda^3}$.

Only the starred terms survive! So, with heating

$$\frac{\partial}{\partial t}\left(\frac{\widehat{\omega}^2}{2}\right) = \overline{\omega'_i \omega'_j s_{ij}} - \overline{\nu\left(\frac{\partial \omega_i}{\partial x_j}\frac{\partial \omega_i}{\partial x_j}\right)} + \left(\beta \boldsymbol{g}.\left(\overline{\boldsymbol{\omega}' \mathrm{x} (\nabla \mathrm{T}')}\right)\right) \text{ --------> } (3)$$

The source for enstrophy is

$$\overline{\beta\boldsymbol{\omega}'.(\mathbf{g}\times\nabla T')} \equiv \beta\mathbf{g}.(\overline{\boldsymbol{\omega}'\times\nabla T'}). \tag{10}$$

Noting that $\beta\nabla T' = -(\nabla\rho')/\rho_{\mathrm{o}}$, and taking $\nabla\rho'$ as of order $\hat{\rho}_c/\lambda_\rho$, where $\hat{\rho}_c$ is (say) the centreline rms of value ρ', and introducing λ_ρ as the Taylor microscale for the density field (although no measurements of λ_ρ are known to the author), the enstrophy source is of order

$$\frac{\mathbf{g}}{\rho_o}\frac{U_c}{\lambda}\frac{\hat{\rho}_c}{\lambda_\rho}, \tag{11}$$

where $\hat{\rho}$ will be determined by the heat release. This term seems to be responsible for the explosive increase in enstrophy found in the BaN simulations, particularly in the spectrum at high wave numbers (see Figure 5f).

VIGOROUSLY CONVECTING CUMULUS CLOUD

Could the sharply crinkled surface of the cloud be due to explosive growth in high wave number turbulent vorticity?

RADIAL DISTRIBUTION OF BAROCLINIC TORQUE

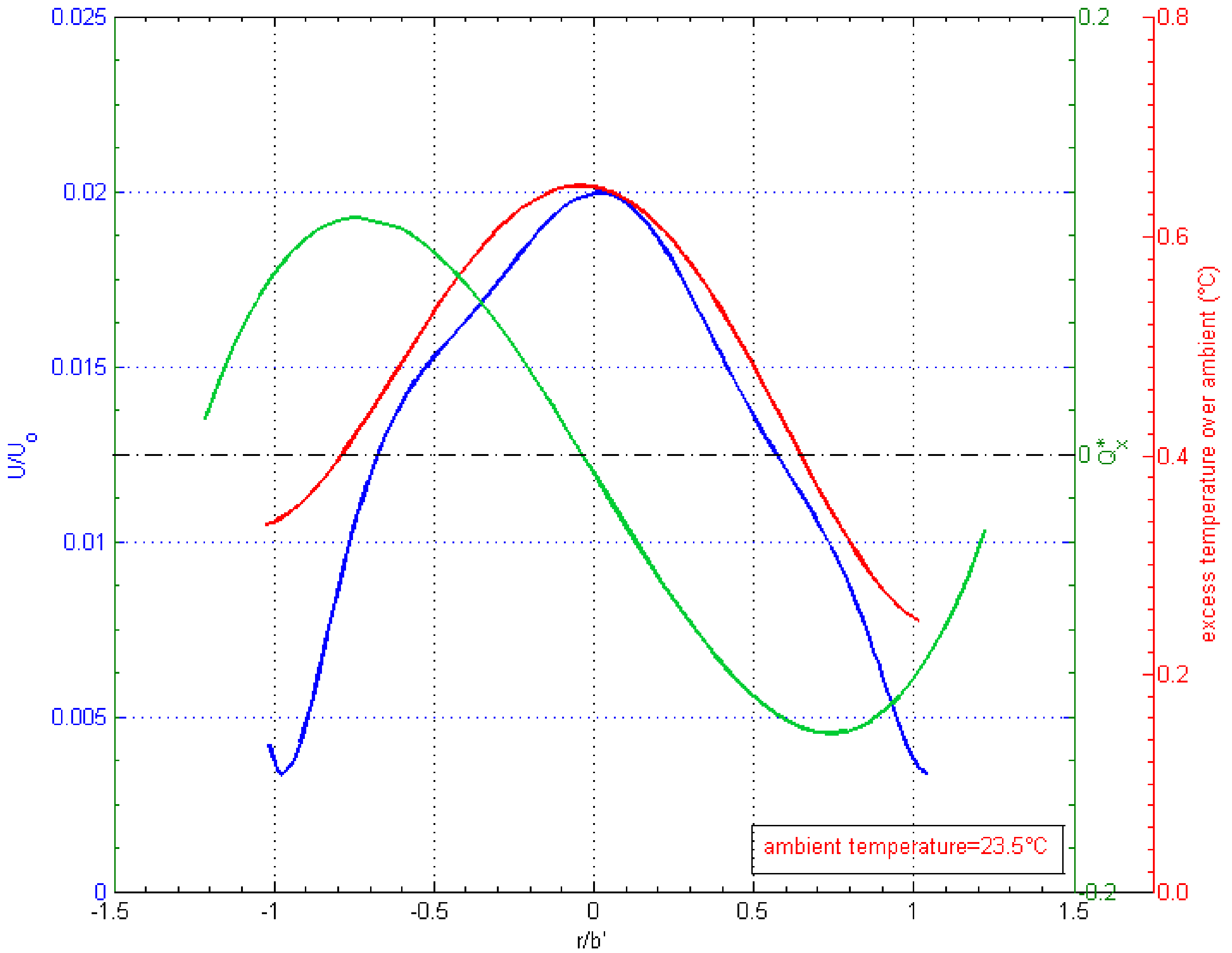

Based on experiments of Agrawal et al. 2004 *IJHMT*

P Kulkarni 2012 JNC Report

RADIAL DISTRIBUTION OF BAROCLINIC TORQUE

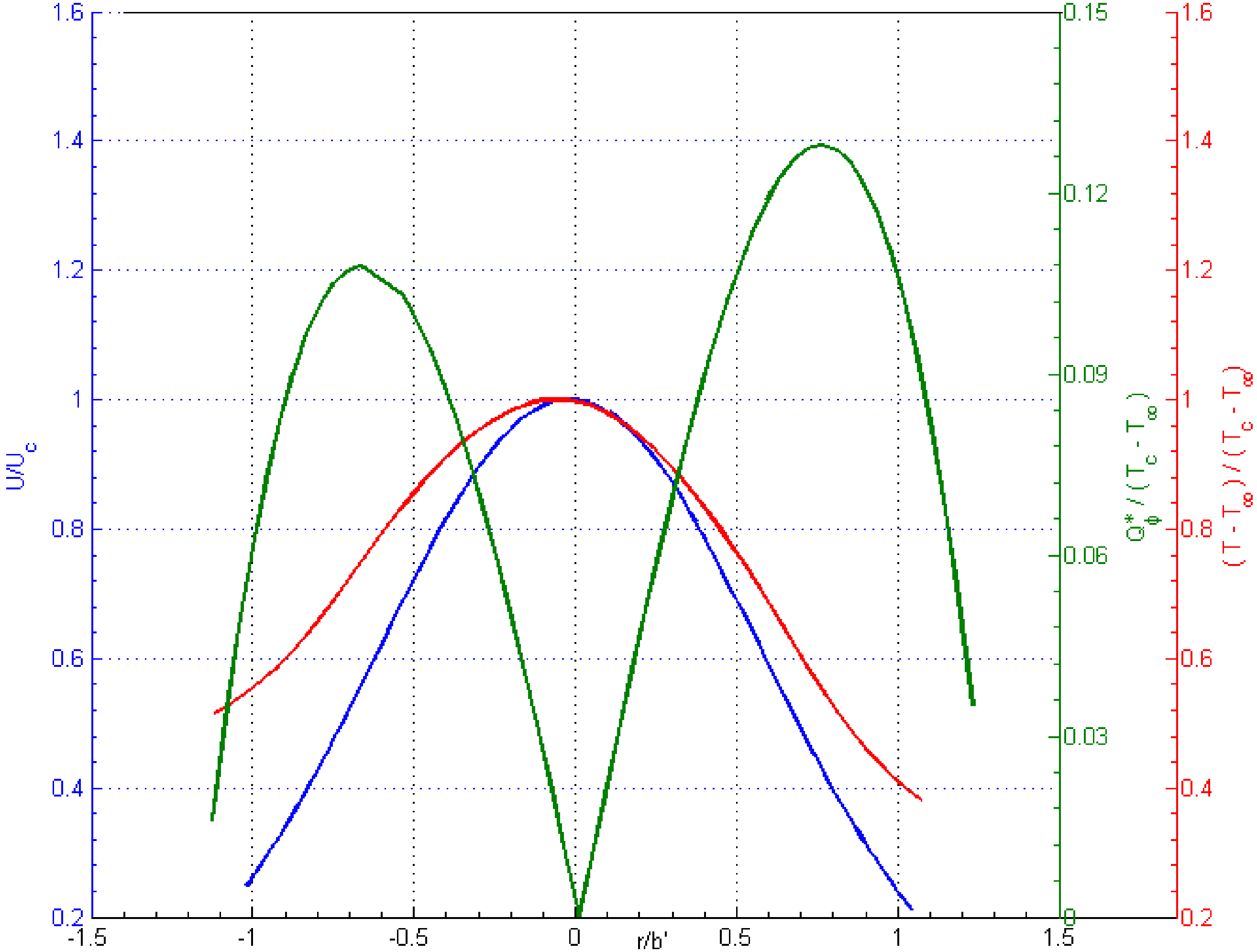

Smoothed data

P Kulkarni 2012
JNC Report

RADIAL DISTRIBUTION OF KINEMATIC BAROCLINIC TORQUE DENSITY

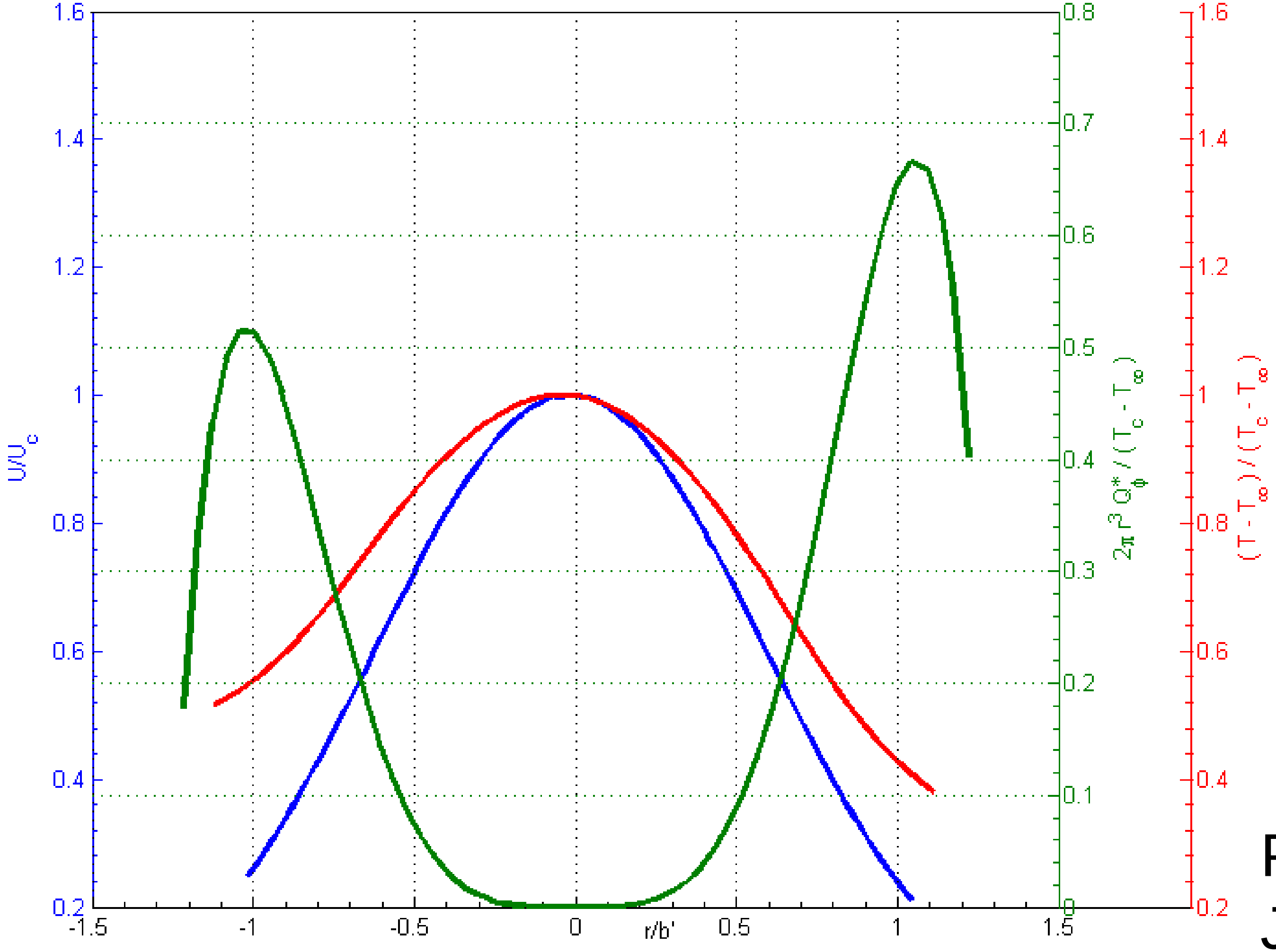

P Kulkarni 2012
JNC Report

WHAT WE NEED

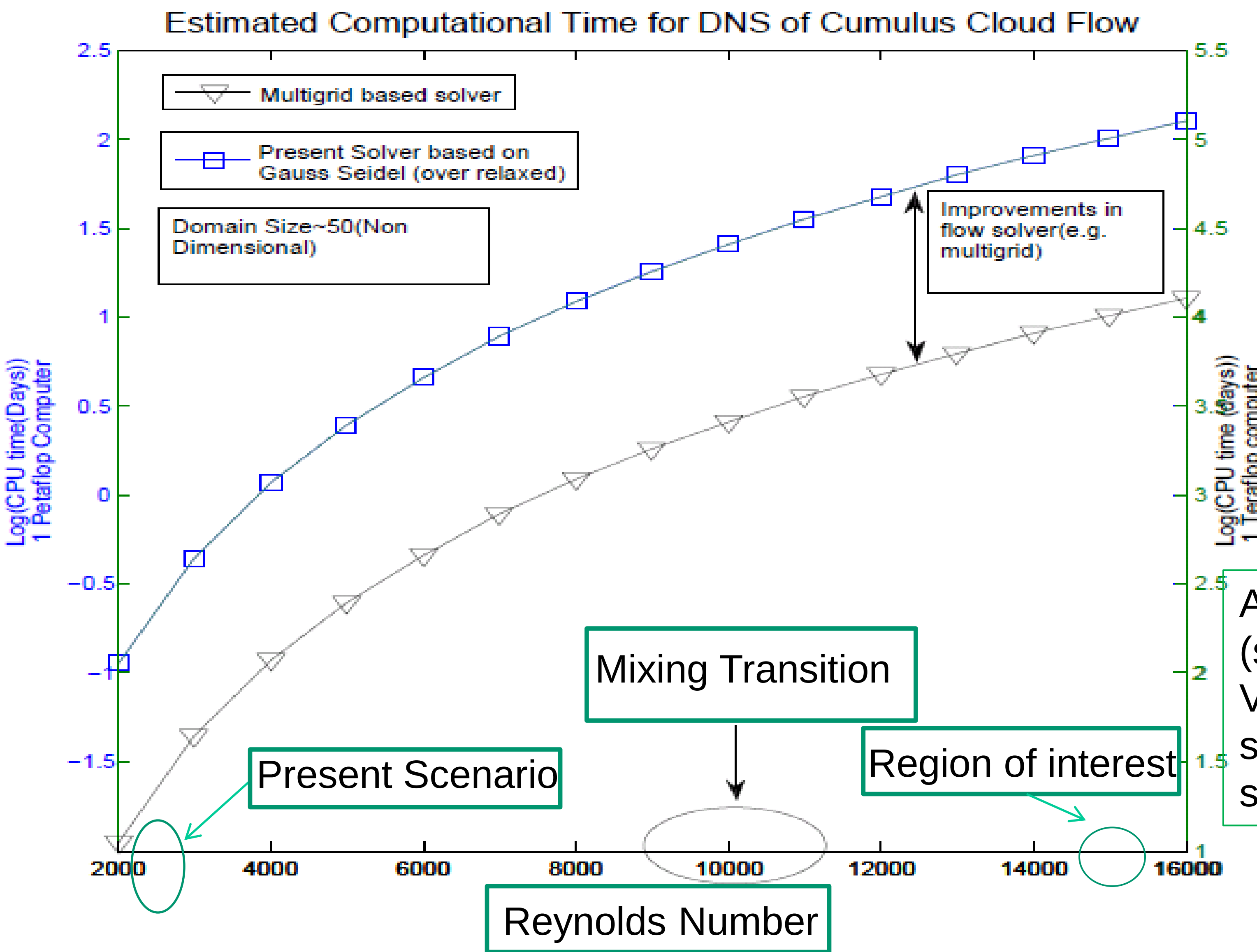

Also : 3D (steoreoscopic) Visualization software and system

CONCLUSION

1. Laboratory and numerical experiments show that a transient diabatic plume offers a suitable flow model for a cumulus cloud, as it can reproduce the form of several species of the genus
2. The entrainment coefficient in steady or transient diabatic plumes shows dramatic variations in space, and large departures from similarity plume values
3. The heating profile in the vertical and its history play a key role in determining the evolution of a cumulus flow through its whole life cycle
4. The baroclinic torque, proportional to the horizontal temperature gradient, provides simple mechanistic explanations for the entrainment characteristics of cumulus flows, and for the sharp crinkly edges seen in a cumulus in early stage of vigorous convection

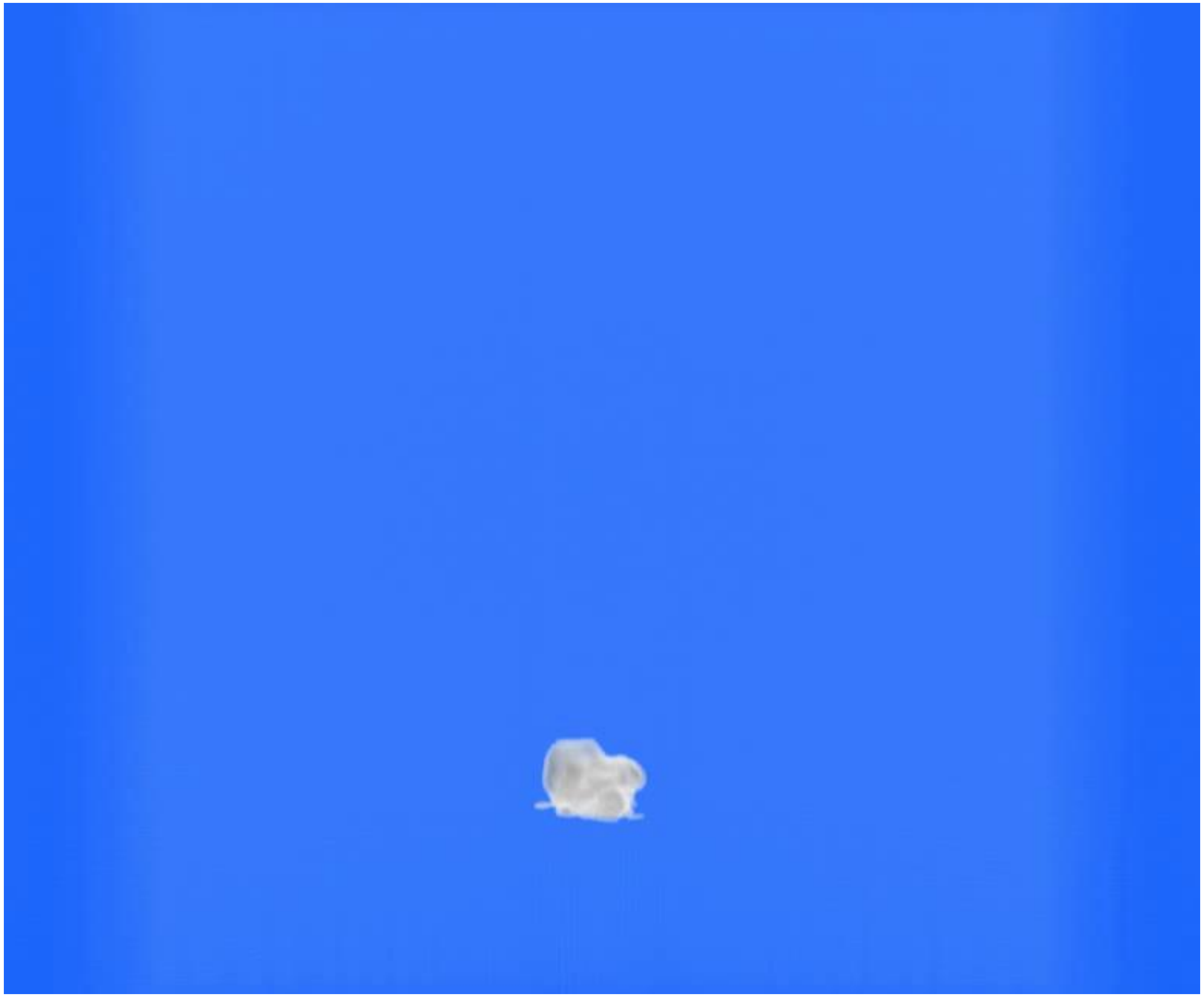

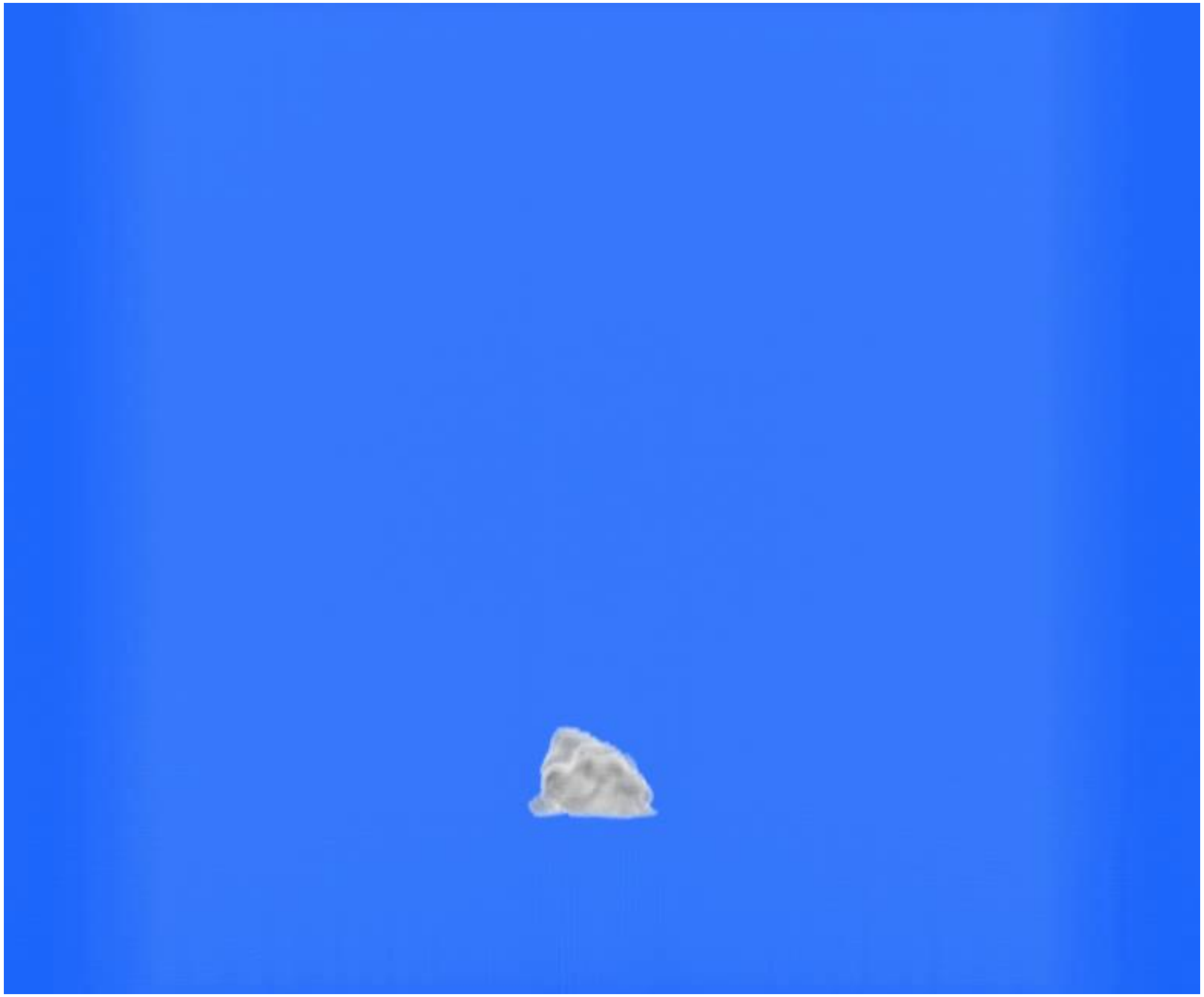

Thank you !

VORTICITY MOVIE – TAP (UNHEATED)

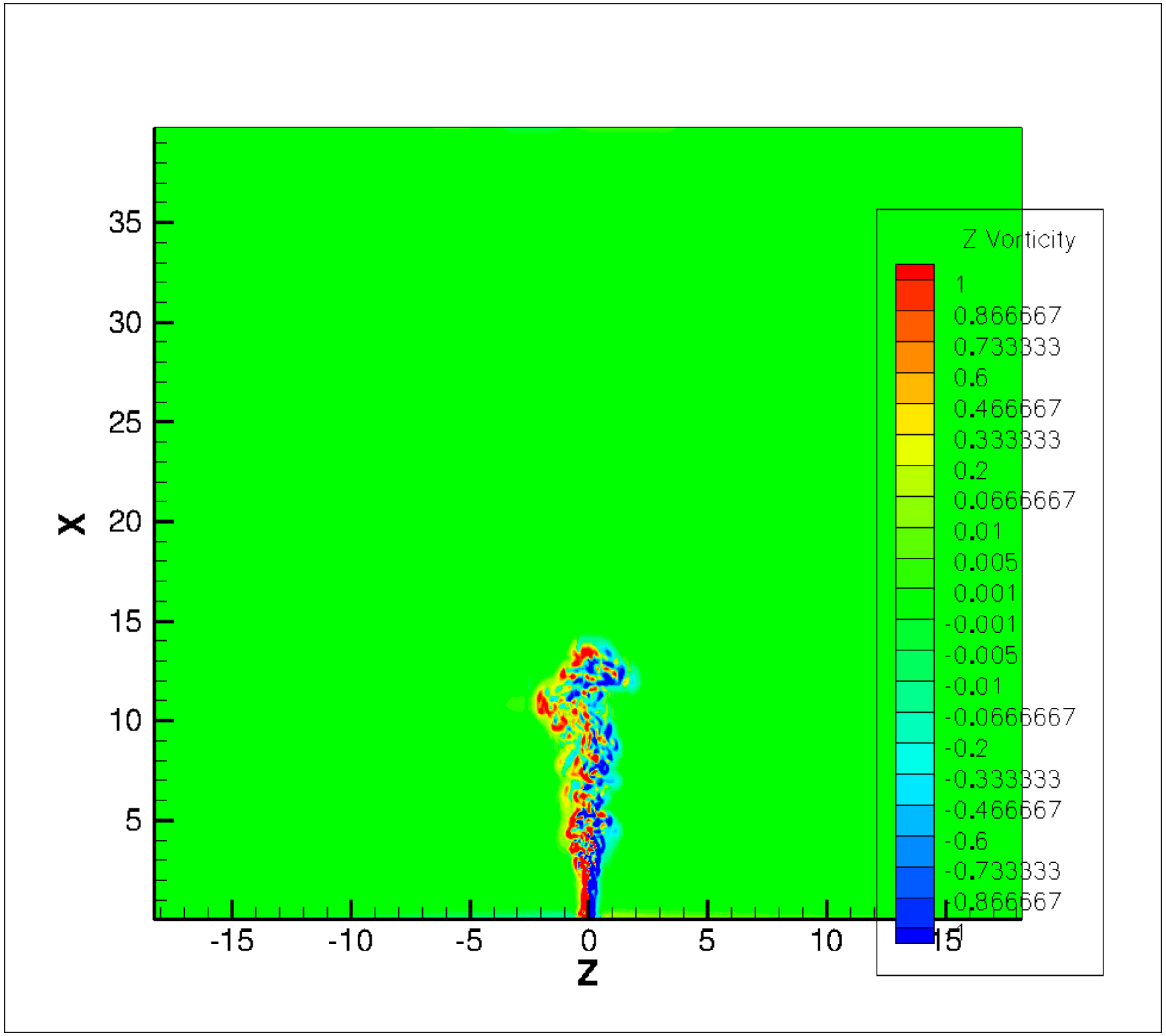

VORTICITY MOVIE – TDP (HEATED)

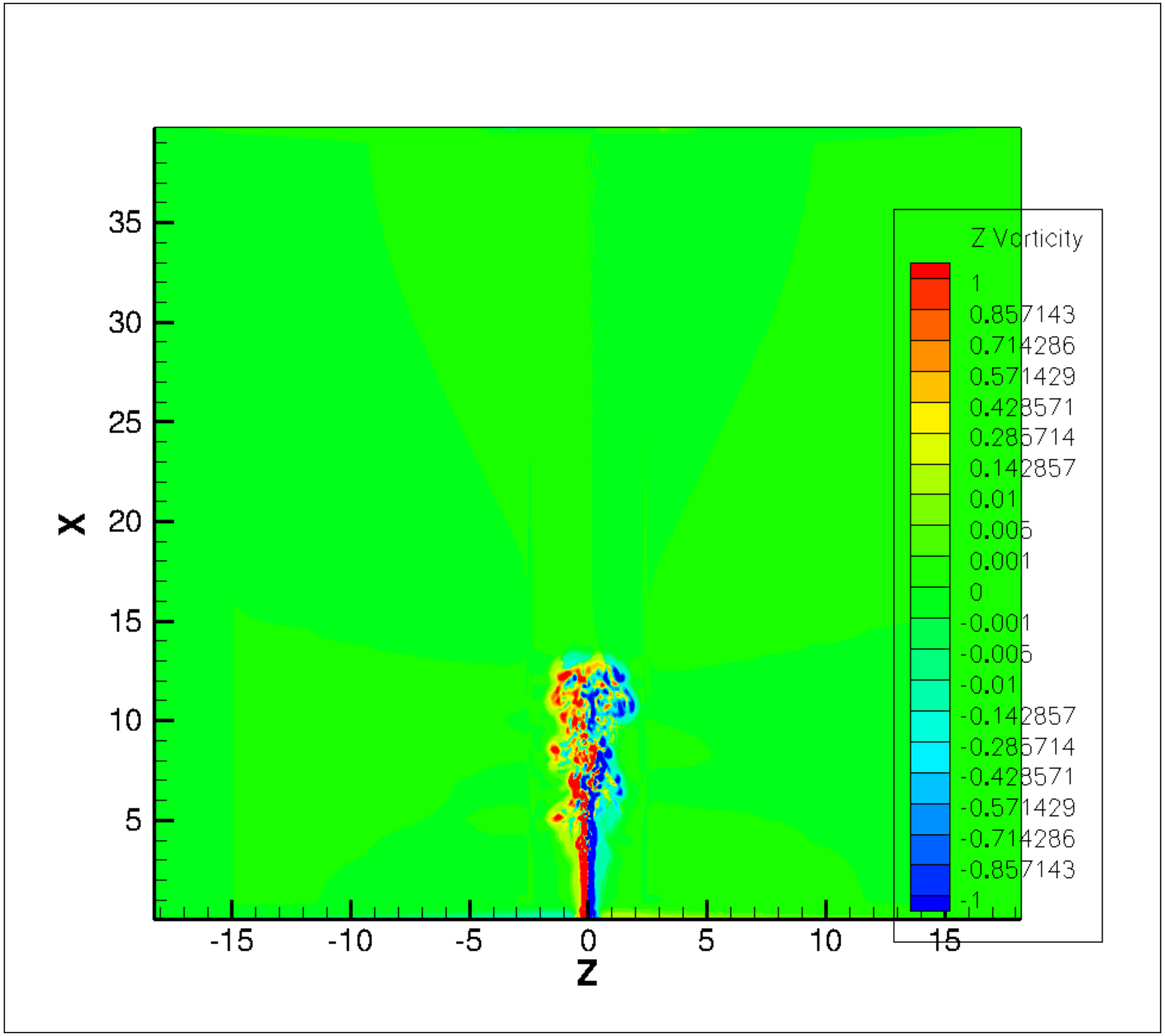

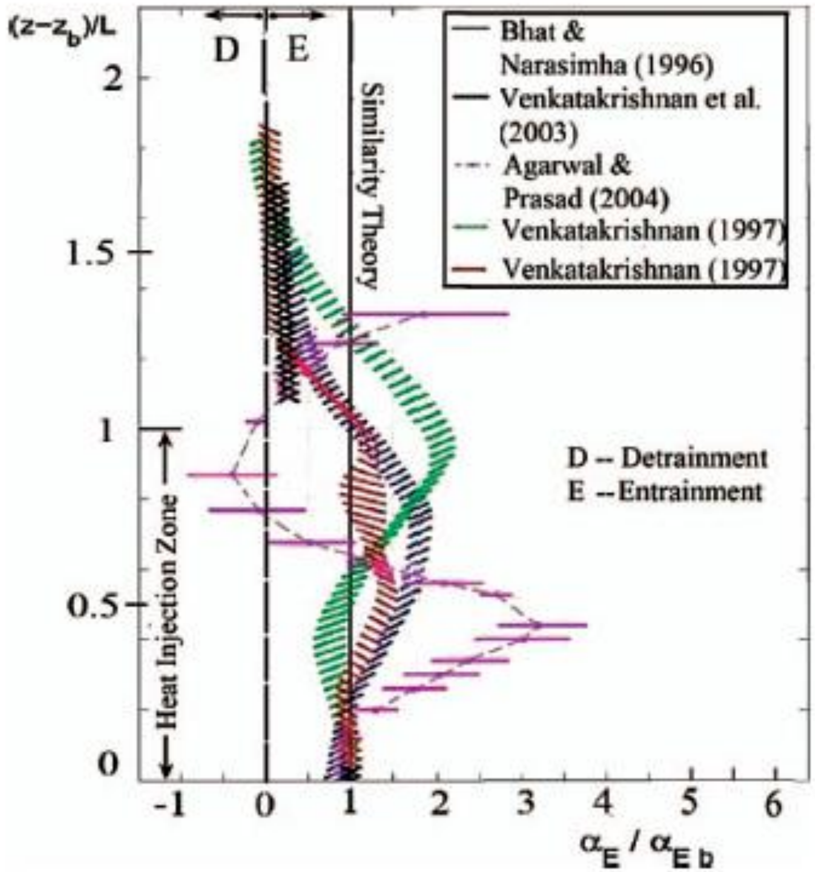

Figure 4. Experimental data available to date on a normalized entrainment coefficient in diabatic jets and plumes. *Sources*: Bhat and Narasimha [40], Venkatakrishnan et al. [46], Agarwal and Prasad [44] and Venkatakrishnan [53]. Based on [39].

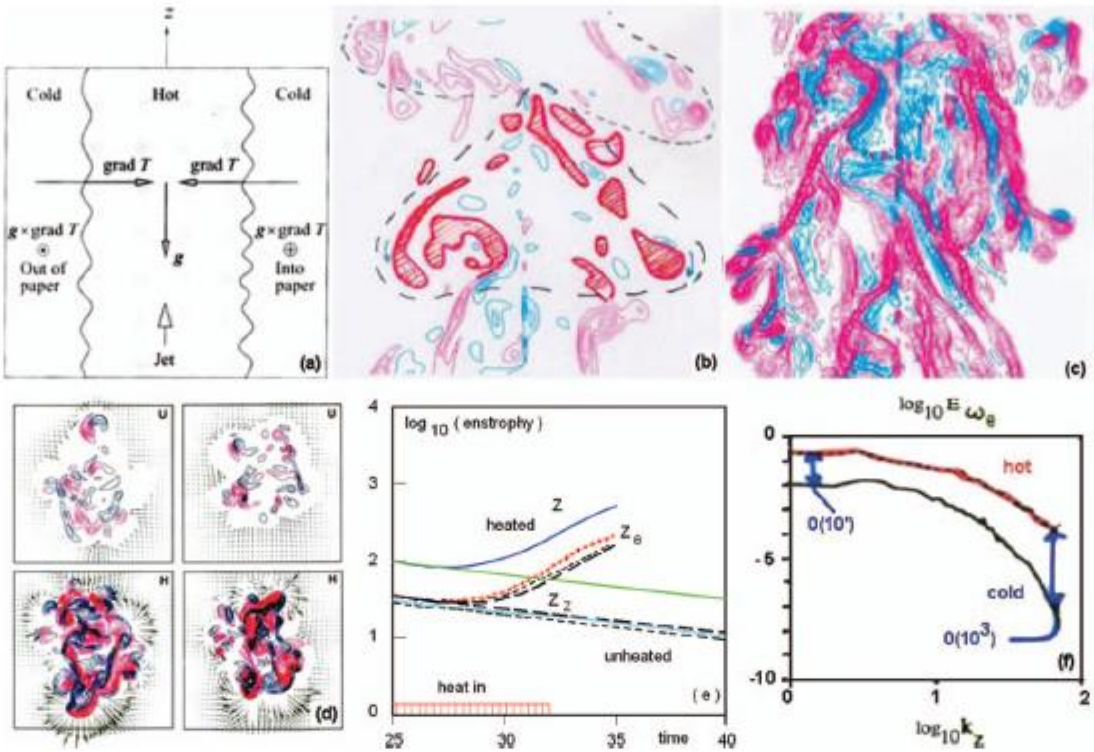

Figure 5. A collage of diagrams summarizing the most striking features of direct numerical solutions of the Navier–Stokes–Boussinesq equations. All data used in the diagrams are from the solutions carried out for BaN [38], but parts of (b), (c) and (d) were not published in [38]. Flow parameters: Re = 1600, Prandtl number Pr = 7, heat release number $G^* = 0.04$. (For definition of G^*, see BaN38, p. 203.) Solutions at $t = 35$, heat injection from $t = 25$ to 32. Vorticity contours at intervals of 0.5; dashed lines negative, solid lines positive. (a) Schematic of temporal flow problem solved, showing directions of gravity, mean temperature gradient and the mean baroclinic torque acting in the azimuthal direction. (b) Azimuthal vorticity contours in an axial section of the non-diabatic jet, showing a coherent structure (situated within the dashed closed curve). Contours start from –0.5. (c) Axial section through a diabatic jet with all other parameters being the same as in (b). (d) Diametral cross-sections showing streamwise vorticity in unheated (top row) and heated (bottom row) jets. (Left) Narrowest cross-section; (right) widest cross-section of flow. (e) Comparison of the evolution of enstrophy in heated (bold lines) and unheated (light lines) jets. (f) Computed spectra of the azimuthal component of the enstrophy for unheated (full line) and heated (dashed line) jets. (a), (e), (f): Reproduced with permission from [38]; (b), (c), (d): Based on work done and reported in [38].

The source for enstrophy is

$$\overline{\beta\omega'.(\mathbf{g}\times\nabla T')} \equiv \beta\mathbf{g}.(\overline{\omega'\times\nabla T'}). \tag{10}$$

Noting that $\beta\nabla T' = -(\nabla\rho')/\rho_o$, and taking $\nabla\rho'$ as of order $\hat{\rho}_c/\lambda_\rho$, where $\hat{\rho}_c$ is (say) the centreline rms of value ρ', and introducing λ_ρ as the Taylor microscale for the density field (although no measurements of λ_ρ are known to the author), the enstrophy source is of order

$$\frac{\mathbf{g}}{\rho_o}\frac{U_c}{\lambda}\frac{\hat{\rho}_c}{\lambda_\rho}, \tag{11}$$

where $\hat{\rho}$ will be determined by the heat release. This term seems to be responsible for the explosive increase in enstrophy found in the BaN simulations, particularly in the spectrum at high wave numbers (see Figure 5f).

Laboratory Simulation: THE PROTECTED CORE*

Ordinary Plume Diabatically Heated Plume

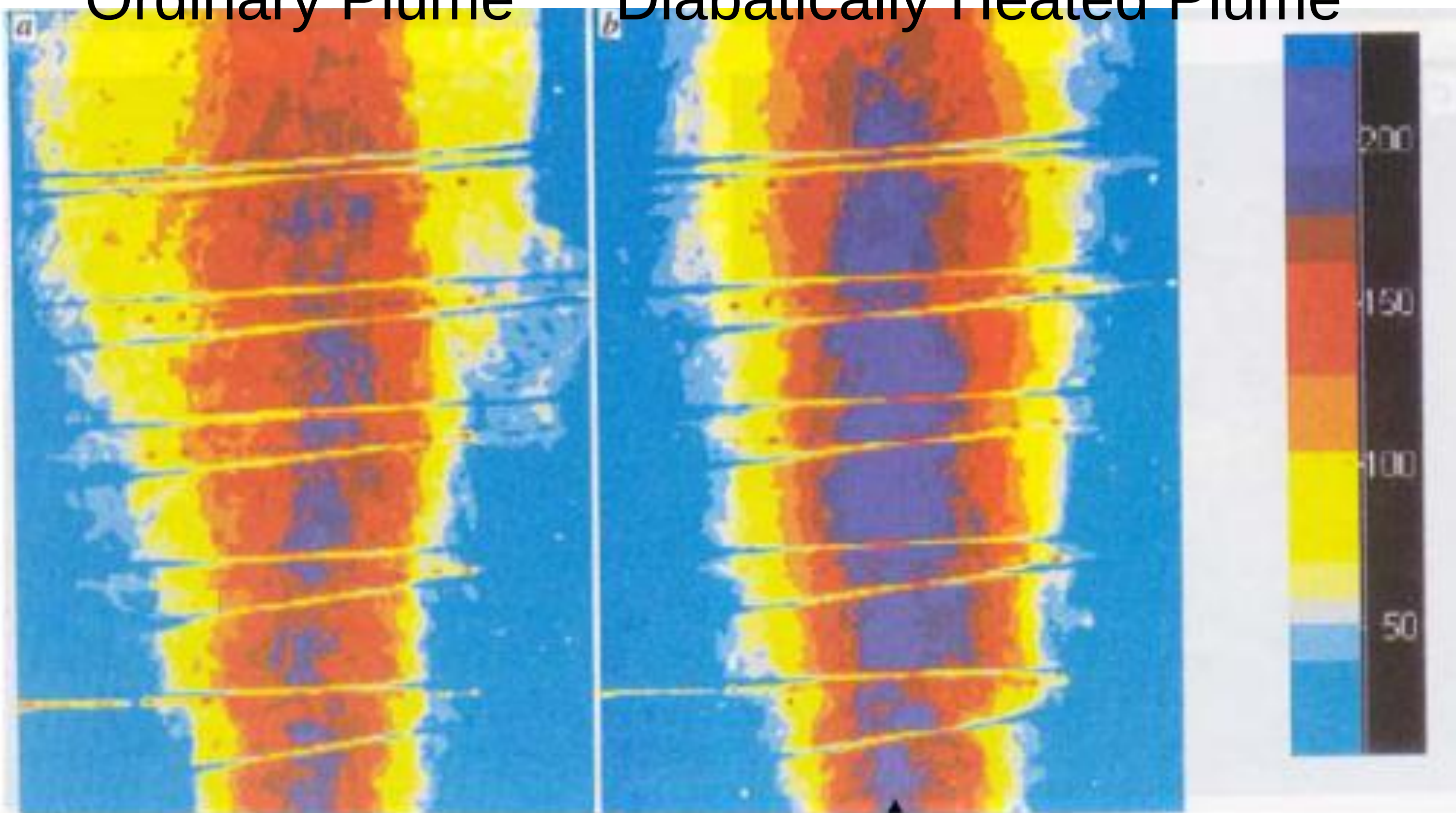

Protected core

Average pictures of dye concentration in vertical cross-sections of the unheated and heated plume. Note*: Little dilution in the core with diabatic heating

* Riehl, Malkus 1958 *Geophysica* Venkatakrishnan et al. 19

Instantaneous vorticity and velocity field

Transient jet

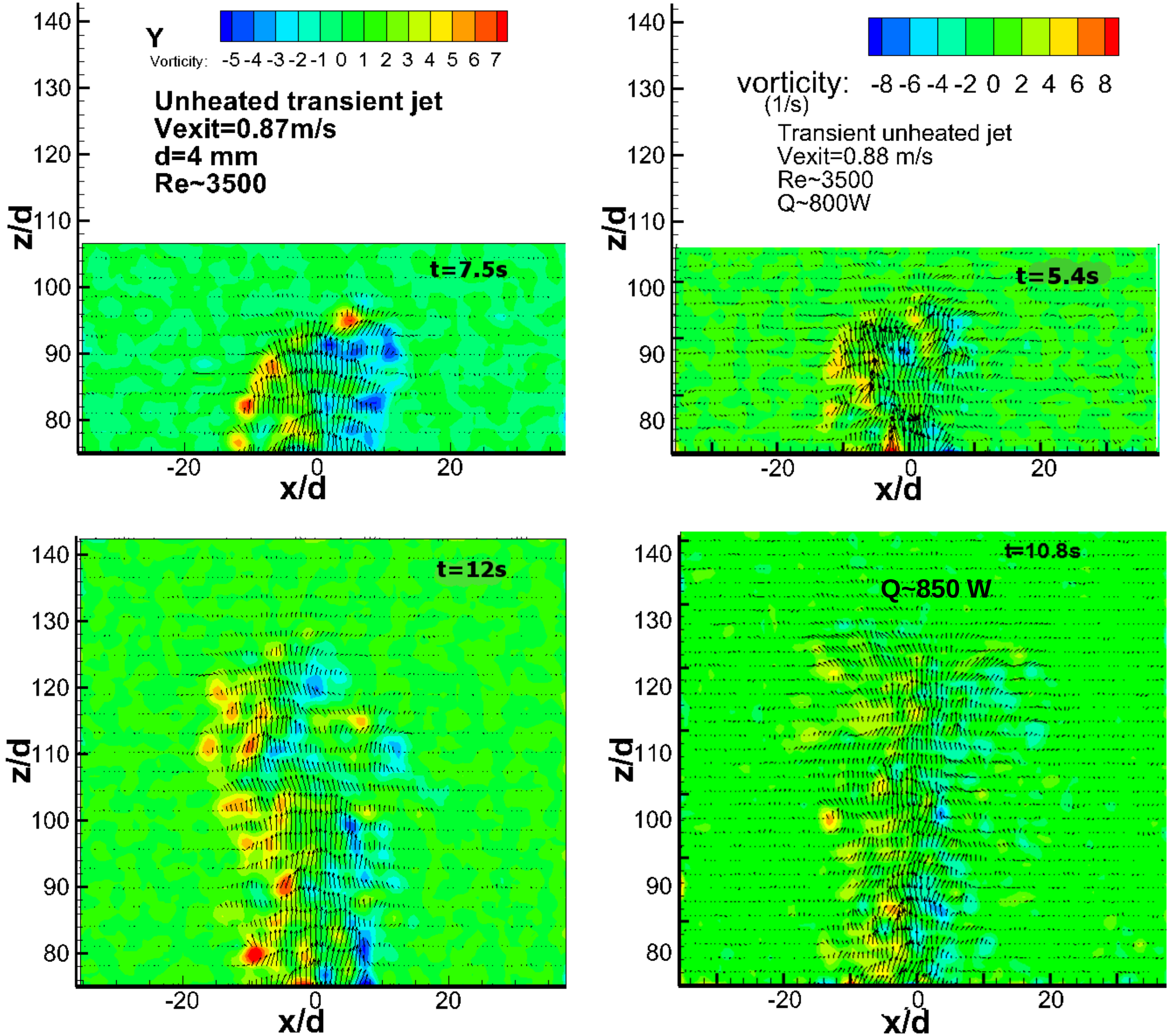

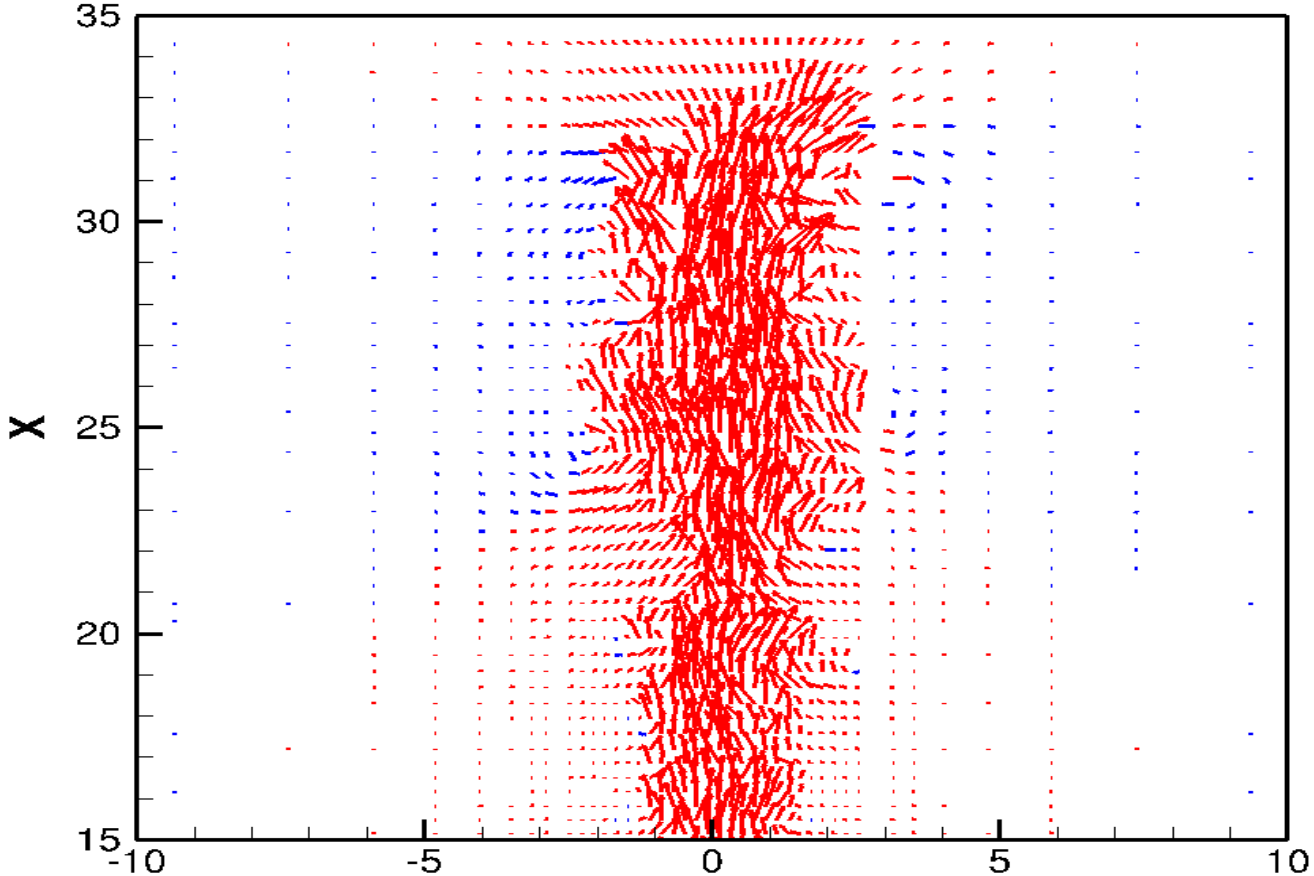

Radial displacement
from the axis

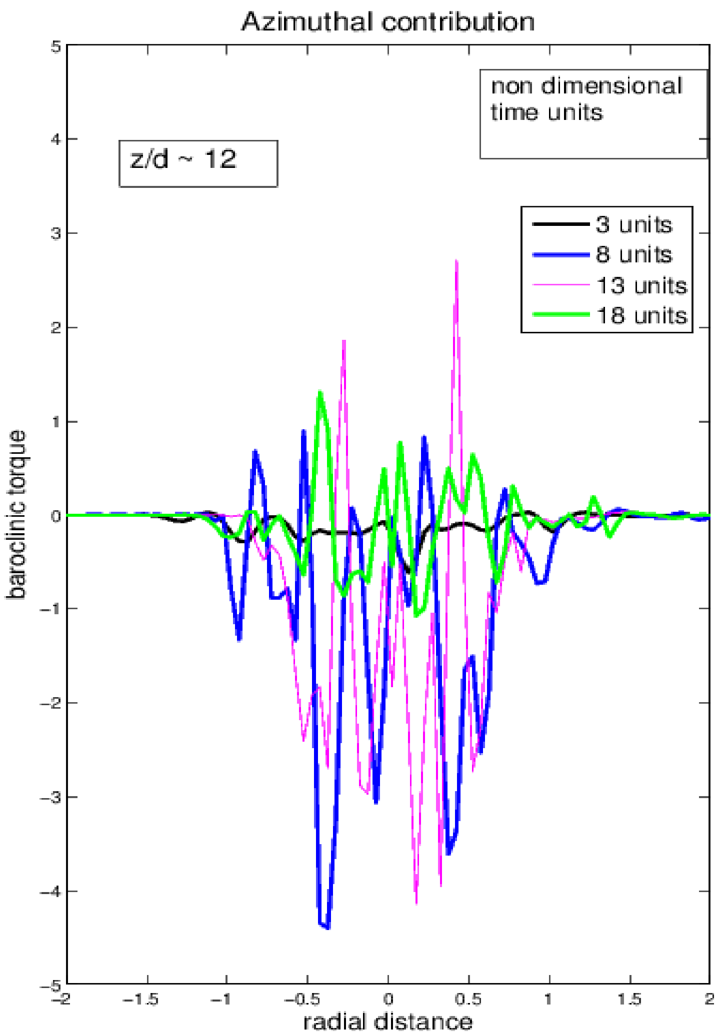
Azimuthal contribution
non dimensional
time units
z/d ~ 12
3 units
8 units
13 units
18 units
baroclinic torque
radial distance
5
4
3
2
1
0
−1
−2
−3
−4
−5
−2
−1.5
−1
−0.5
0
0.5
1
1.5
2

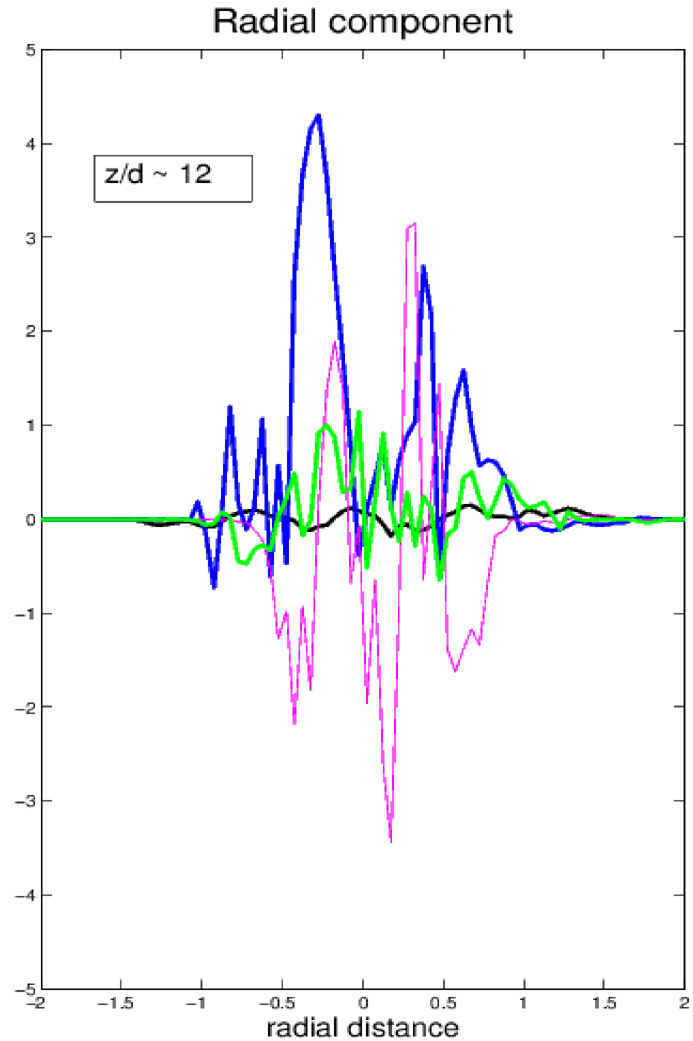
Radial component
z/d ~ 12
radial distance
5
4
3
2
1
0
−1
−2
−3
−4
−5
−2
−1.5
−1
−0.5
0
0.5
1
1.5
2

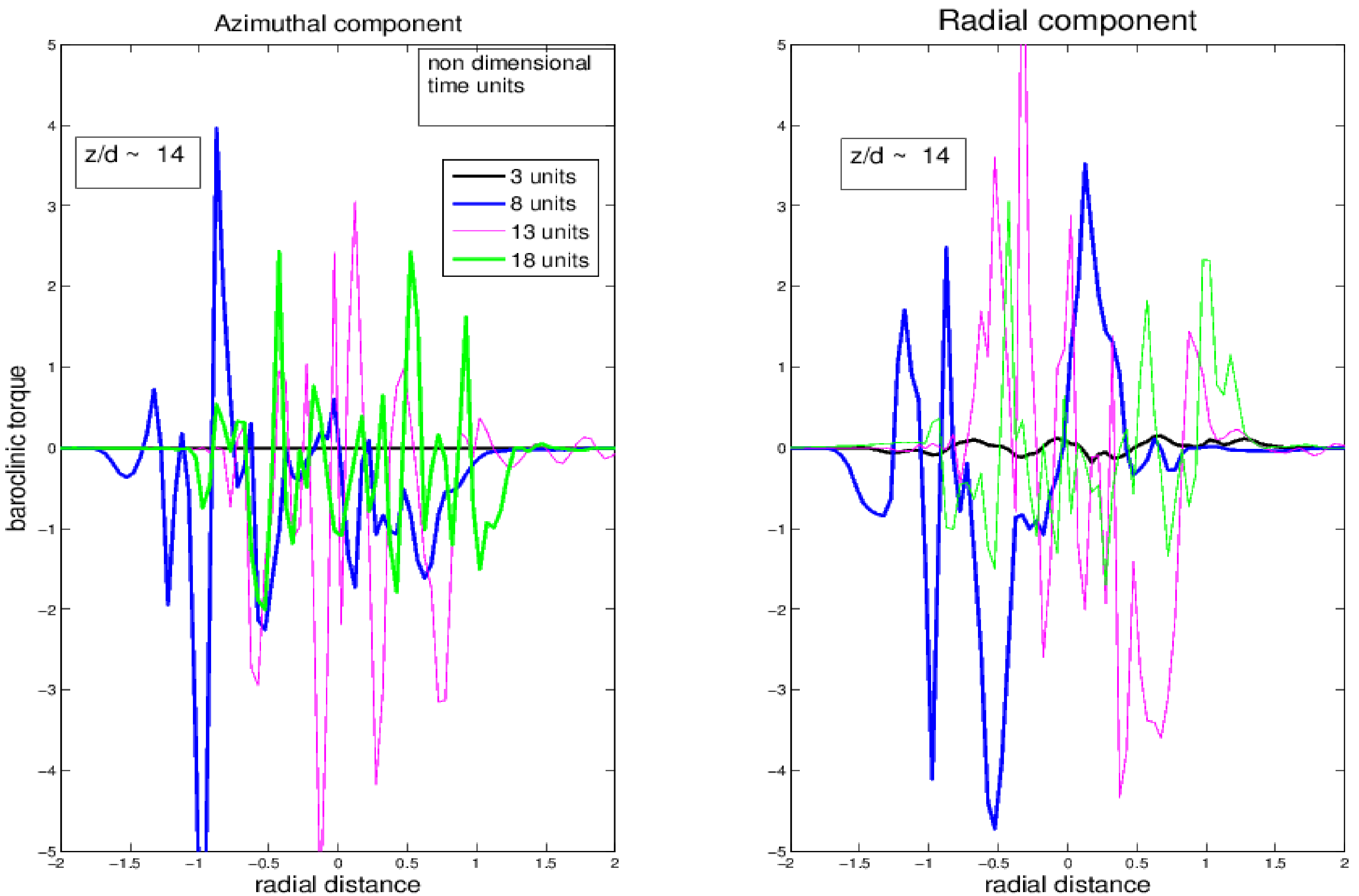
Azimuthal component
non dimensional
time units
z/d ~ 14
3 units
8 units
13 units
18 units
baroclinic torque
radial distance
Radial component
z/d ~ 14
radial distance

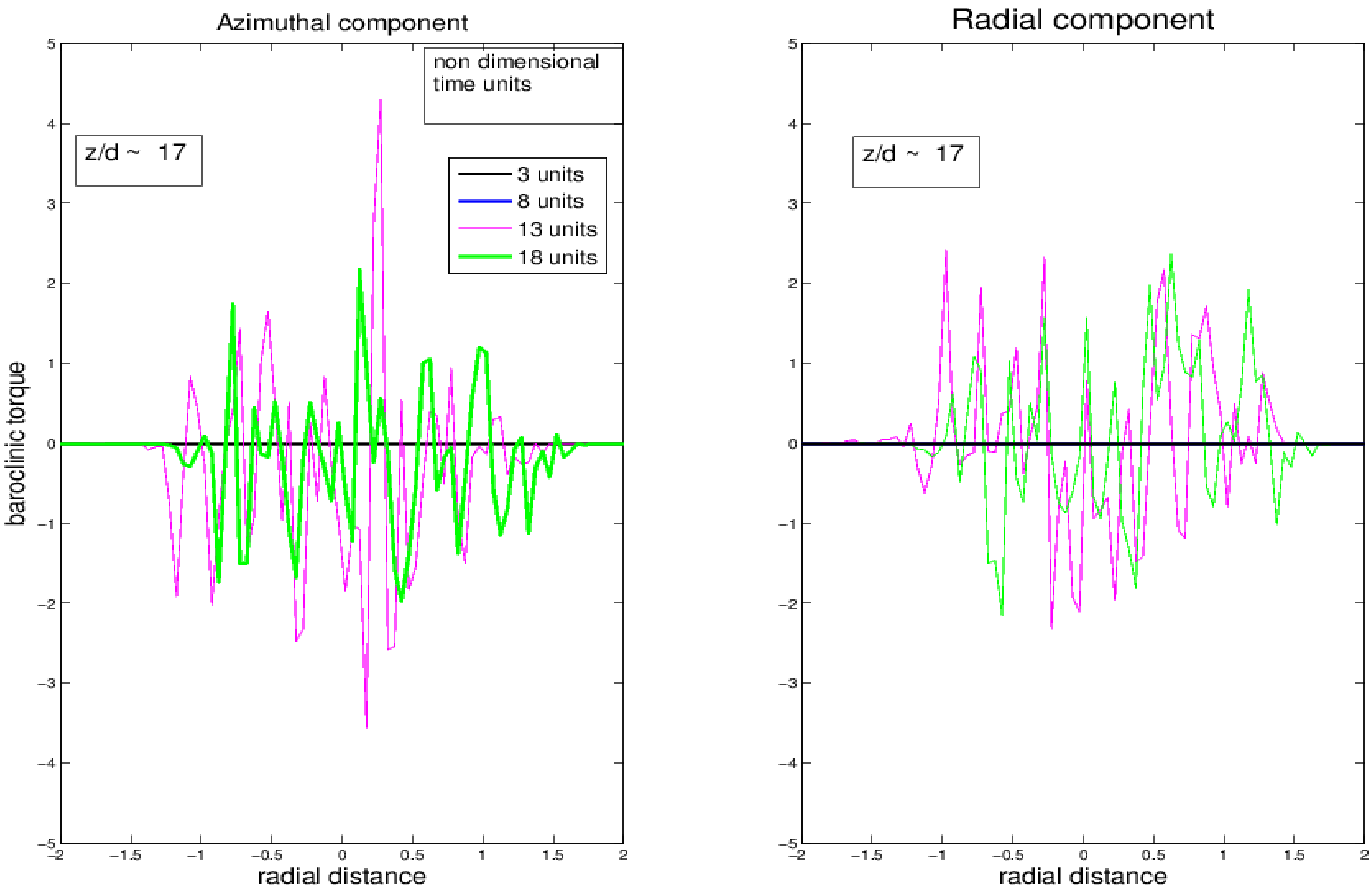
Azimuthal component
non dimensional
time units
z/d ~ 17
3 units
8 units
13 units
18 units
baroclinic torque
radial distance
Radial component
z/d ~ 17
radial distance